

A Novel Noise-Aware Classical Optimizer for Variational Quantum Algorithms

Jeffrey Larson^a, Matt Menickelly^a, and Jiahao Shi^b

^aMathematics and Computer Science Division, Argonne National Laboratory.

jmlarson@anl.gov, mmenickelly@anl.gov

^bIndustrial and Operations Engineering Department, University of Michigan.

jiahaos@umich.edu

Abstract

A key component of variational quantum algorithms (VQAs) is the choice of classical optimizer employed to update the parameterization of an ansatz. It is well recognized that quantum algorithms will, for the foreseeable future, necessarily be run on noisy devices with limited fidelities. Thus, the evaluation of an objective function (e.g., the guiding function in the quantum approximate optimization algorithm (QAOA) or the expectation of the electronic Hamiltonian in variational quantum eigensolver (VQE)) required by a classical optimizer is subject not only to stochastic error from estimating an expected value but also to error resulting from intermittent hardware noise. Model-based derivative-free optimization methods have emerged as popular choices of a classical optimizer in the noisy VQA setting, based on empirical studies. However, these optimization methods were not explicitly designed with the consideration of noise. In this work we adapt recent developments from the “noise-aware numerical optimization” literature to these commonly used derivative-free model-based methods. We introduce the key defining characteristics of these novel noise-aware derivative-free model-based methods that separate them from standard model-based methods. We study an implementation of such noise-aware derivative-free model-based methods and compare its performance on demonstrative VQA simulations to classical solvers packaged in `scikit-quant`.

1 Introduction

Variational quantum algorithms (VQAs) form a class of quantum algorithms and are a leading method of experimentation for quantum computing researchers and practitioners [1]. VQAs have quantum circuit representations that are relatively simple and short and are therefore particularly well suited for near-term quantum computers, which have limited qubits and are prone to errors [2, 3]. The “variational” nature of VQAs comes from the manner in which VQAs combine classical optimization methods with quantum information techniques. The core idea behind VQAs is to use a quantum computer to evaluate a parameterized quantum circuit; the final quantum state returned

by a VQA therefore depends on a given set of parameters. These parameters are adjusted by some classical numerical optimization algorithm that seeks the optimum of a well-designed and problem-specific cost function. Two of the most common VQAs are the quantum approximate optimization algorithm (QAOA) [3] and the variational quantum eigensolver (VQE) [4], which differ in their application and form. QAOA has shown promise for solving binary optimization problems, for example, MaxCut variants [5, 6] and low autocorrelated binary sequences [7] problems, where as VQE has shown promise in performing quantum simulations to identify ground state energies of complex molecules [8]. The efficacy and flexibility of VQAs have piqued the interest of researchers in chemistry [9–11], materials science [12], and machine learning [1].

In this manuscript we are particularly interested in the classical numerical optimization method that forms a critical part of a VQA. While some work suggests exploiting *parameter shifts* [13] to compute gradients with respect to the parameters, quantum circuits for computing these gradients are generally very large and hence far more prone to errors resulting from hardware noise. Some exploratory work in gradient-based classical optimizers for the VQA setting was performed by [14–19]. These gradient-based optimizers offer improved theoretical convergence over derivative-free methods ([20]). However, in the near term where gate depths are prohibitive, the classical numerical optimization methods used to optimize VQA parameters will likely continue to have access only to cost function values. Given the complexity of the cost functions for these quantum systems, the employed optimization methods must be robust and efficient in navigating a landscape that is generally nonconvex and periodic [21]. This challenge, central to our motivations in this paper, is compounded by the fact that quantum measurements are inherently probabilistic; this means that the cost function values used in VQA are generally only statistical estimates. In particular, one is limited to sampling repeated measurements (called *shots*) of the output state of a quantum circuit; because most cost functions are expectations, a sample average of shot measurements typically yields an unbiased estimate of the cost function. However, these estimates necessarily introduce stochastic noise (in addition to, or separate from, any hardware noise) into the optimization process.

1.1 Existing Methods

With the consideration of practically unattainable gradients, practitioners typically use methods for derivative-free optimization (DFO) [22] as the classical optimizer in a VQA. By derivative-free methods we refer to any optimization method that does not require any derivative information to be supplied by the user or the cost function oracle. For example, the software package `scikit-quant` [23] wraps a variety of derivative-free optimization solvers that the authors found to perform well on several benchmark VQE problems.

As discussed, the optimization problem solved on the classical computer is inherently stochastic. Despite this, the quantum computing community has largely found DFO methods that are explicitly for optimizing stochastic responses to be far less efficient than their counterparts for deterministic responses; for example, none of the solvers wrapped in `scikit-quant` are intended for stochastic optimization, by the standard definition of stochastic optimization. However, as is obvious in

theory and is indeed observed in practice, any method designed for a deterministic problem will never resample a cost function at the same parameter setting twice. As a result, deterministic methods are certain to eventually “get stuck”; that is, they will fail to find improvement resulting from small perturbations of the circuit parameters. This “stuckness” is likely to happen when the noise becomes relatively large compared with the change in the cost function resulting from a parameter perturbation suggested by the methods.

Some of the most successful optimization methods for DFO problems (VQA or otherwise) are slight modifications to the model-based trust-region (MBTR) framework [24], with notable implementations having been developed by Michael Powell, including the popular BOBYQA [25]. MBTR methods construct and update a quadratic model of the objective function over a dynamically adjusted trust region, typically a norm ball of fixed radius in the parameter space. MBTR methods allow for efficient approximation of the overall objective function’s behavior, thereby guiding the optimization process more reliably, even in the absence of explicit gradient information. The method’s quadratic models are interpolatory; these models are especially useful when the signal from a noisy response is large relative to the noise. If the signal-to-noise ratio becomes small, however, the interpolatory models are likely not to model the response but rather provide a model of noise. In this low-signal setting, MBTR methods are likely to become stuck. However, MBTR methods empirically make reasonable progress for as long as the signal-to-noise ratio remains high.

1.2 Our Contribution

In this work we seek to explicitly account for the observation that theoretically, and practically, MBTR methods perform best when the signal-to-noise ratio remains high. We accomplish this goal by developing what we call a *noise-aware* MBTR method. By noise-aware, we broadly refer to any method that effectively requires an *estimate* of the noise level present in the function evaluation. We currently leave the meaning of noise level intentionally vague, but for intuition, noise level could refer to any of the following:

- a deterministic bound on the absolute value of noise,
- the standard error when one employs sample means to estimate an expectation value, or
- the noise level of a deterministically noisy function, as employed in [26],

among other quantities. We note in particular that we do not label our method a *stochastic* MBTR because, for instance, of the three examples presented above, only the second example assumes anything stochastic about the function being estimated. In the VQA setting, this choice is motivated by the practical concern that observations of circuit evaluations on a near-term quantum computer are the result not only of a stochastic calculus but also of hardware noise. There is generally no reason to believe that hardware noise satisfies distributional assumptions as pleasant as unbiasedness or parameter independence. Moreover, from a theoretical perspective, the analysis of stochastic optimization methods tends to focus on (non)asymptotic convergence rates as a primary

concern. For convergence analyses of various stochastic MBTR methods, see, for example, [27–32]. All of these methods effectively assume that, in the presence of stochastic noise, one must sample the objective function in each iteration k at a rate like $\mathcal{O}(1/\Delta_k^4)$, where Δ_k is a trust-region radius. Because the theoretical convergence of an MBTR method requires $\Delta_k \rightarrow 0$, this sampling rate can quickly become infeasible in practice. As a result, the stochastic optimization methods suggested by these analyses focus on long-term convergence, often at the expense of efficiency in the number of function evaluations spent while satisfying a fixed budget.

Therefore, we seek to provide the best possible theoretical convergence results for a *noise-aware* MBTR method. We aim to achieve this by building on recent results in what we would call noise-aware optimization. Of particular note are [33] and [34], which provide convergence analyses for trust-region frameworks given explicit access to an estimate of a noise level. The definitions of “noise level” differ between these two reference works; we believe that the framework in [34] provides a bit more flexibility that allows the results to be especially appropriate in the VQA setting. The results of both [33] and [34] can be characterized as providing a neighborhood of convergence for an optimization method given a reasonable estimate of the noise level. Thus, instead of trying to achieve arbitrary accuracy (which, for instance, would require an insurmountable number of samples in a stochastic setting), the analysis provides a worst-case rate of convergence to a solution of “best possible” accuracy, given the noise level. The primary achievement of this manuscript is to take the noise-aware trust-region framework of [34] and, through careful consideration of interpolation model construction, yield a *practical implementation of a noise-aware MBTR method*. The convergence of our method will follow immediately by algorithmically ensuring that the interpolation models satisfy certain properties that are assumed in [34].

1.3 Paper Organization

The outline of the manuscript is as follows. Section 2 develops the problem setting, and Section 2.1 discusses the chosen noise model suitable for VQAs. Section 2.2 presents a general noise-aware trust-region algorithm from the literature that we will build upon, and Section 2.3 presents some of its theoretical properties. Section 3 presents our novel method for noise-aware optimization, and Section 4 analyzes the convergence properties of its sequence of iterates. Section 5 presents numerical results for our novel algorithm on a selection of noisy optimization problems. Section 6 concludes with open questions for further investigation.

2 Setting

Given a computational ansatz, let a quantum circuit be parameterized by $\theta \in \mathcal{R}^d$. We aim to solve the optimization problem

$$\text{minimize } f(\theta) : \theta \in \mathcal{R}^d, \tag{1}$$

where $f : \mathcal{R}^d \rightarrow \mathcal{R}$ denotes some objective function (e.g., a guiding function in QAOA or the energy of the Hamiltonian in VQE).

We first discuss, in [Section 2.1](#), a particular choice of noise model from recent literature that appears to be appropriate for the noisy VQA setting. A suitable trust-region algorithm for the minimization of objective functions subscribing to this noise model was also recently proposed, and we present it in [Section 2.2](#). In [Section 2.3](#) we summarize results concerning the asymptotic performance of this trust-region algorithm.

2.1 A Noise Model

Motivated by the role of the classical optimizer in the VQA setting, we consider a noise setting similar to that investigated in Cao et al. [\[34\]](#). In particular, we suppose that our access to an underlying objective function $f : \mathcal{R}^d \rightarrow \mathcal{R}$ is through what Cao et al. [\[34\]](#) refers to as a “stochastic zeroth-order oracle” (of one of two types):

Definition 1. *Let ξ denote a random variable that may or may not depend on the optimization variables θ . We say $\tilde{f}(\theta, \xi)$ is a zeroth-order oracle for f provided for all $x \in \mathcal{R}^d$, the error quantity*

$$e(\theta, \xi) = \tilde{f}(\theta, \xi) - f(\theta) \tag{2}$$

satisfies at least one of two conditions:

Type 1. (Deterministically bounded noise) *There exists a constant $\epsilon_f \geq 0$ such that $|e(\theta, \xi)| \leq \epsilon_f$ for all realizations of ξ .*

Type 2. (Independent subexponential noise) *There exist constants $\epsilon_f \geq 0$ and $c > 0$ such that*

$$\mathbb{P}_\xi [|e(\theta, \xi)| > t] \leq \exp(c(\epsilon_f - t)) \quad \forall t \geq 0. \tag{3}$$

We remark that the random variable ξ in [Definition 1](#) should be considered exogenous in the sense that an optimization algorithm accessing \tilde{f} cannot provide an input ξ . Hence, for ease of notation, we will denote the noisy evaluations of f as $\tilde{f}(\theta)$ throughout this manuscript. We additionally remark that while, for generality, [Definition 1](#) is stated in terms of random variables, the definition does not preclude noisy deterministic functions; in that case, one can trivially assign some Dirac distribution to ξ , and the definition is still meaningful. To provide context, one can interpret [eq. \(3\)](#) as saying that the errors exhibit a subexponential tail (with rate determined by c); moreover, [eq. \(3\)](#) suggests that there are no restrictions on the distribution of errors of magnitude within ϵ_f . Many commonly used and naturally occurring probability distributions fall within this definition.

We believe the assumption that a quantum computer’s output exhibits the properties of a zeroth-order oracle is reasonable. For example, in QAOA, a single shot of the output of the quantum circuit corresponds to one of combinatorially many binary vectors, which are then evaluated through the objective function of a combinatorial optimization problem on the classical device. The objective function used by the classical optimizer, in turn, is essentially an average of Bernoulli variables (one variable for each binary solution) weighted by the original combinatorial problem’s objective values.

If one supposes that the combinatorial problem is well defined, and because Bernoulli variables have bounded (finite) support, the error ϵ_f is always trivially deterministically bounded in QAOA and is a [Type 1](#) error as we have defined.

Of course, such a trivial deterministic bound is loose to the point of uselessness. However, using Bernstein inequality, one can show that the distribution of errors of the finitely supported \tilde{f} will yield c in [eq. \(3\)](#) that scales linearly in the shot count (that is, the subexponential rate of decay is proportionally faster). Given this observation, we may replace ϵ_f with the standard deviation σ of the distribution described by $\tilde{f}(\theta, \xi)$, where ξ describes the randomness associated with a given number of shots.

We are additionally attracted to the noise model defined in [Definition 1](#) in the VQA setting because of its nonparametric flexibility. The definition itself does not specify what the noise distribution ought to be but essentially assumes, via conditions on the tail of the noise distribution, only that the variance of $\tilde{f}(\theta)$ is defined and that there exist bounds on higher moments of $\tilde{f}(\theta)$.

We also find this noise model attractive for VQA because of intermittent hardware noise, which remains a salient difficulty in near-term quantum devices. Owing to the nonparametric assumption, even if a quantum device “drifts” over time [\[35\]](#), the noise model is sufficiently flexible to describe a sum of stochastic error (as previously discussed) and hardware error. While the “variance” (and higher moments) of hardware noise is not easily quantifiable, allowing a sufficiently large ϵ_f in the deterministically bounded regime of [Definition 1](#) can potentially encapsulate hardware noise. This interpretation lends credence to the use and purported convergence guarantees of algorithms based on zeroth-order oracles, like the one we will describe now.

2.2 A Noise-Aware Trust-Region Algorithmic Framework

We begin by restating the general first-order trust-region algorithm of Cao et al. [\[34\]](#)[[Algorithm 1](#)] in [Algorithm 1](#); our statement is identical up to changes in notation. For a complete statement of [Algorithm 1](#), we require one additional definition, which must be carefully handled in derivative-free optimization.

Definition 2. *Let ξ denote a random variable. We say $g(\theta, \xi)$ is a first-order oracle for $\nabla f(\theta)$ provided there exist $\kappa_{eg} \geq 0$ and $\epsilon_g \geq 0$ such that for any given $\theta \in \mathcal{R}^d$, for any given $\Delta > 0$, and for any given probability $p_1 \in [0.5, 1]$,*

$$\mathbb{P}_\xi [\|g(\theta, \xi) - \nabla f(\theta)\| \leq \epsilon_g + \kappa_{eg}\Delta] \geq p_1. \tag{4}$$

The random variable ξ may or may not depend on θ and Δ .

Given access to a zeroth-order oracle (see [Definition 1](#)) and a first-order oracle (see [Definition 2](#)), convergence results for [Algorithm 1](#) may be proven.

Algorithm 1: General framework for noise-aware optimization

Input: starting point θ_0 ; initial trust-region radius $\Delta_0 > 0$; trust-region parameters

$\eta_1, \eta_2, \gamma \in (0, 1)$, tolerance parameter $r \geq 2\epsilon_f$, probability parameter p_1 , bound on model Hessians $\kappa_{\text{bmh}} \geq 0$, constant $\kappa_{\text{fcd}} \in (0, 1]$

1 Evaluate $\tilde{f}(\theta)$ if not previously evaluated.

2 **for** $k = 0, 1, 2, \dots$ **do**

3 Compute model gradient g_k via first-order oracle with input θ_k, p_1 , and Δ_k

4 Let H_k be a model Hessian satisfying $\|H_k\| \leq \kappa_{\text{bmh}}$

5 Construct a local quadratic model

$$m_k(s) = \tilde{f}(\theta_k) + g_k^T s + s^T H_k s \quad (5)$$

6 Compute s_k as an approximate minimizer of $\{\min m_k(s) : s \in \mathcal{B}(0, \Delta_k)\}$, such that s_k satisfies

$$m_k(\theta_k) - m_k(\theta_k + s_k) \geq \frac{\kappa_{\text{fcd}}}{2} \|g_k\| \min \left\{ \frac{\|g_k\|}{\|H_k\|}, \Delta_k \right\} \quad (6)$$

7 Evaluate $\tilde{f}(\theta_k + s_k)$ from zeroth-order oracle as in [Definition 1](#).

8 Compute

$$\rho_k = \frac{\tilde{f}(\theta_k) - \tilde{f}(\theta_k + s_k) + r}{m_k(0) - m_k(s_k)} \quad (7)$$

9 **if** $\rho_k \geq \eta_1$ **then**

$$\text{Set } \theta_{k+1} = \theta_k + s_k \text{ and } \Delta_{k+1} = \begin{cases} \gamma^{-1} \Delta_k & \text{if } \|g_k\| \geq \eta_2 \Delta_k \\ \gamma \Delta_k, & \text{if } \|g_k\| < \eta_2 \Delta_k \end{cases}$$

10 **else**

11 | Set $\theta_{k+1} = \theta_k$ and $\Delta_{k+1} = \gamma \Delta_k$.

2.3 Preliminary Assumptions and Analysis

Under reasonable assumptions, Cao et al. [34][Theorems 4.11 and 4.18] demonstrate that in both the deterministically bounded noise regime and the subexponential noise regime, the probability of exceeding $\mathcal{O}(1/\epsilon^2)$ iterations of [Algorithm 1](#) to find an ϵ -stationary solution to [eq. \(1\)](#) decays exponentially in the exceedance; ϵ is a function of ϵ_f and ϵ_g .

We start by making the following assumptions.

Assumption 1. *The objective function f is continuously differentiable. That is, the gradient ∇f is $L_{\nabla f}$ -Lipschitz continuous on \mathcal{R}^d and satisfies*

$$\|\nabla f(\theta^{(1)}) - \nabla f(\theta^{(2)})\| \leq L_{\nabla f} \|\theta^{(1)} - \theta^{(2)}\|$$

for all $(\theta^{(1)}, \theta^{(2)}) \in \mathcal{R}^d \times \mathcal{R}^d$.

Assumption 2. The function f is lower bounded by f_{\inf} .

Assumption 3. For all $k = 0, 1, \dots$, $\|H_k\| \leq \kappa_{\text{bhm}}$, where $\kappa_{\text{bhm}} > 0$.

We state intentionally simplified versions of two main results of Cao et al. [34], which provide the number of iterations T needed to ensure (with high probability) that within the first T iterations, the event $\{\|\nabla f(\theta_k)\| \leq \epsilon\}$ occurs.

Theorem 1. Suppose Assumptions 1–3 are satisfied. Suppose we have access to a zeroth-order oracle of Type 1 with parameter ϵ_f and a first-order oracle with parameters κ_{eg}, ϵ_g , and p_1 . Let $\{\Theta_k\}$ denote the sequence of random variables with realizations $\{\theta_k\}$ generated by Algorithm 1. There exists κ , independent of $\epsilon_f, \epsilon_g, p_1$ but dependent on κ_{eg} , such that given any

$$\epsilon > \kappa \left(\sqrt{\frac{\epsilon_f}{2p_1 - 1}} + \epsilon_g \right),$$

it holds that

$$\mathbb{P} \left[\min_{0 \leq k \leq T-1} \|\nabla f(\Theta_k)\| \leq \epsilon \right] \geq 1 - \exp(-\mathcal{O}(T))$$

for any $T \in \mathcal{O}\left(\frac{1}{\epsilon^2}\right)$.

Theorem 2. Suppose that Assumptions 1–3 are satisfied. Suppose we have access to a zeroth-order oracle of Type 2 with parameters ϵ_f and c and a first-order oracle with parameters κ_{eg}, ϵ_g , and p_1 . Define $p_0 = 1 - 2 \exp(c(\epsilon_f - r/2))$. Let $\{\Theta_k\}$ denote the sequence of random variables with realizations $\{\theta_k\}$ generated by Algorithm 1. There exists κ , independent of $\epsilon_f, \epsilon_g, p_1$ but dependent on κ_{eg} , such that given any

$$\epsilon > \kappa \left(\sqrt{\frac{\epsilon_f + 1/c}{2p_0 + 2p_1 - 3}} + \epsilon_g \right),$$

it holds that

$$\mathbb{P} \left[\min_{0 \leq k \leq T-1} \|\nabla f(\Theta_k)\| \leq \epsilon \right] \geq 1 - 2 \exp(-\mathcal{O}(T)) - \exp(-ct/4)$$

for any $T \in \mathcal{O}\left(\frac{1}{\epsilon^2}\right)$ and any $t > 0$.

Remark 1. While we encourage the reader to study Cao et al. [34][Theorems 4.11 & 4.18] for a complete description of the constants that we have deliberately hidden in $\mathcal{O}(T)$ and $\mathcal{O}(1/\epsilon^2)$, we remark that, as one might intuit, the $\mathcal{O}(T)$ rate in the exponentially decaying probability decreases in ϵ_f , and the $\mathcal{O}\left(\frac{1}{\epsilon^2}\right)$ term increases with both the initial optimality gap $f(\theta_0) - f_{\inf}$ and the Lipschitz constant $L_{\nabla f}$. When $\epsilon_f = \epsilon_g = 0$, Theorem 1 reduces to something resembling the first-order convergence result for a standard derivative-free trust-region algorithm; see, for example, Conn et al. [24][Chapter 10]. For theoretical soundness, we set r to be any value larger than $2\epsilon_f$. When $r < 2\epsilon_f$, ρ_k could be dominated by the noise and the algorithm may fail to make progress. Since the lower bounds on ϵ in Theorem 1 and Theorem 2 depend on r , $r = 2\epsilon_f$ is the theoretically optimal choice of r , provided ϵ_f was exactly knowable.

3 A Practical Noise-Aware Derivative-Free Algorithm Based on Algorithm 1

While Algorithm 1 provides an invaluable framework for analyzing DFO methods, it does not lend itself immediately to a practical algorithm for DFO. In particular, Algorithm 1 does not detail how to construct a first-order oracle for computing g_k or how to choose model Hessians H_k . Cao et al. [34] suggest using linear interpolation of noisy function values for the first-order oracle, similar to the approach analyzed by Berahas et al. [36]. Our approach aligns with this line of reasoning but is further motivated by two practical considerations. First, we aim to go beyond linear interpolation models to also minimum Frobenius norm quadratic interpolation models. (This extension is certainly not new and is the subject of Conn et al. [24][Chapter 5].) Compared to linear interpolation models, minimum Frobenius norm models are more complex and generally model the true objective with greater accuracy when the objective is nonlinear; this typically leads to more per-iteration objective decrease. Additionally, minimum Frobenius norm models do not require as many samples as quadratic interpolation models to construct. Second, and more important, because we often employ model-based methods for optimizing computationally expensive objectives in derivative-free optimization, we do not want to generate a new set of interpolation points on every iteration. Rather, we prefer to judiciously reuse previously evaluated points and their corresponding (noisy) function evaluations. Especially in the noisy setting, this merits a careful reexamination of known results concerning the geometry of interpolation sets and algorithmic methods for ensuring geometric constraints are satisfied in practice. In addition, we impose a lower bound on a sampling radius when we select points for model construction, in order to ensure that the error between the true gradient and the model gradient is controlled. Section 3.1 focuses on precisely establishing these algorithmic controls.

3.1 Geometry of Interpolation Sets

At every iteration $k \in \{0, 1, \dots\}$ of our derivative-free trust-region algorithm, there exists an incumbent iterate θ_k (that is also a trust-region center). In each iteration, a set of distinct points $\mathcal{X} = \{x^0 = \theta_k, x^1, \dots, x^p\} \subset \mathcal{R}^d$ is selected; the algorithm ensures that the noisy function \tilde{f} is evaluated at each $x \in \mathcal{X}$. A model is constructed such that it interpolates the noisy function \tilde{f} at each $x \in \mathcal{X}$, and this model is intended to approximate the objective function near θ_k .

In this work we will focus on minimum Frobenius norm quadratic interpolation models, which are appropriate in the setting of budget-constrained (expensive) derivative-free optimization. We consider the space of all quadratic polynomials in \mathcal{R}^d ; a suitable basis for this space is given by the union of the degree-zero and degree-one monomials $\{1, x_1, x_2, \dots, x_d\}$ and the degree-two monomials $\{x_1^2, \dots, x_d^2, x_1x_2, x_1x_3, \dots, x_1x_n, \dots, x_{n-1}x_n\}$. Vectorizing these two sets as $\mu(x) \in \mathcal{R}^{d+1}$ and $\nu(x) \in \mathcal{R}^{d(d+1)/2}$ respectively, we see that any degree-two polynomial, and hence any quadratic interpolation model, can be expressed as

$$m(x) = \alpha^T \mu(x) + \beta^T \nu(x), \tag{8}$$

for $\alpha \in \mathcal{R}^{d+1}$ and $\beta \in \mathcal{R}^{d(d+1)/2}$.

We assume throughout that the interpolation set \mathcal{X} has cardinality $p \in [d+1, (d+1)(d+2)/2]$. Define

$$\tilde{f}(\mathcal{X}) = \left[\tilde{f}(x^0), \tilde{f}(x^1), \dots, \tilde{f}(x^p) \right]^\top, \quad (9)$$

where $\tilde{f}(x^i)$ represents noisy evaluations of $f(x^i)$ for $i = 0, 1, \dots, p$. Enforcing $m(x^i) = \tilde{f}(x^i)$ for $i = 0, 1, \dots, p$ is tantamount to solving

$$\begin{bmatrix} M_{\mathcal{X}} \\ N_{\mathcal{X}} \end{bmatrix}^T \begin{bmatrix} \alpha \\ \beta \end{bmatrix} = \tilde{f}(\mathcal{X}), \quad (10)$$

where we define $M_{\mathcal{X}} \in \mathcal{R}^{(d+1) \times |\mathcal{X}|}$ and $N_{\mathcal{X}} \in \mathcal{R}^{d(d+1)/2 \times |\mathcal{X}|}$, by $M_{i,j} = \mu_i(x^j)$ and $N_{i,j} = \nu_i(x^j)$, respectively. Note that eq. (10) may not admit a unique solution since $|\mathcal{X}| \leq (d+1)(d+2)/2$. We will focus on solutions to the interpolation problem eq. (10) that are of minimum norm with respect to the vector β . That is, we seek (α, β) that solve

$$\min \left\{ \frac{1}{2} \|\beta\|^2 : M_{\mathcal{X}}^T \alpha + N_{\mathcal{X}}^T \beta = \tilde{f}(\mathcal{X}) \right\}. \quad (11)$$

The solution to eq. (11) is a quadratic polynomial whose Hessian matrix is of minimum Frobenius norm, since $\|\beta\| = \|\nabla_{xx}^2 m(x)\|_F$. The KKT conditions for eq. (11) can be written as

$$\begin{bmatrix} N_{\mathcal{X}}^T N_{\mathcal{X}} & M_{\mathcal{X}}^T \\ M_{\mathcal{X}} & 0 \end{bmatrix} \begin{bmatrix} \lambda \\ \alpha \end{bmatrix} = \begin{bmatrix} \tilde{f}(\mathcal{X}) \\ 0 \end{bmatrix} \quad (12)$$

with $\beta = N_{\mathcal{X}} \lambda$. We make the observation that to guarantee eq. (12) will yield a unique solution, we must have that both $\text{rank}(M_{\mathcal{X}}) = d+1$ and $N_{\mathcal{X}}^T N_{\mathcal{X}}$ is positive definite for all $u \in \mathcal{R}^d$ such that $M_{\mathcal{X}} u = 0$.

Although relatively expensive compared with, for instance, the heuristic employed in POUNDers (see Wild [37] for details), we find that careful geometry maintenance is critical to the performance of a derivative-free model-based optimization method in the noisy setting. Recalling Definition 1, we aim to ensure that, given $\Delta > 0$, the model gradient g defined by α in eq. (8) satisfies eq. (4) for some values of ϵ_g , κ_{eg} , and p_1 . Demonstrating such a result requires careful consideration of the geometry of \mathcal{X} . We begin by introducing the concept of Lagrange polynomials associated with \mathcal{X} .

Definition 3. *Given a set $\mathcal{X} = \{x^0, x^1, \dots, x^p\} \subset \mathcal{R}^d$ of interpolation points, we define the minimum Frobenius norm Lagrange polynomials associated with \mathcal{X} as the set of polynomials $\{\ell_i(x) = \alpha_i^\top \mu(x) + \beta_i^\top \nu(x) : i = 0, 1, \dots, p\}$ with coefficients (α_i, β_i) chosen such that, for each i , (α_i, β_i) is the solution to eq. (11) when the function f in the right-hand side in the constraint is replaced with the indicator function for x^i .*

It is straightforward to demonstrate that the minimum Frobenius norm model $m(x)$ in eq. (8) is expressible via a linear combination of minimum Frobenius norm Lagrange polynomials, that is,

$$m(x) = \sum_{i=0}^p f(x^i) \ell_i(x). \quad (13)$$

Moreover, denoting the matrix in the left-hand side of eq. (12) by $W_{\mathcal{X}}$, it is clear from the definition of minimum Frobenius norm Lagrange polynomials that each (α_i, β_i) defining the polynomials may be computed directly from the columns of $W_{\mathcal{X}}^{-1}$. In particular, the last $d + 1$ entries of the i th column of $W_{\mathcal{X}}^{-1}$ define α_i . Also, by considering the constraints in the quadratic dual program to eq. (11), one may derive that the quadratic term of $\ell_i(x)$ described by β_i is a weighted sum of rank-one matrices,

$$\nabla^2 \ell_j(x) = \sum_{i=0}^p [W_{\mathcal{X}}^{-1}]_{j+1,i} (x^i - x^0)(x^i - x^0)^\top.$$

With computable expressions for the minimum Frobenius norm Lagrange polynomials associated with a set \mathcal{X} in hand, the following definition of Λ -poisedness is easily stated.

Definition 4. *We say that \mathcal{X} is poised in the minimum Frobenius norm sense provided $W_{\mathcal{X}}$ is nonsingular.*

Definition 5. *Let $\Lambda > 0$, and let a set $B \subset \mathcal{R}^d$ be given. A set $\mathcal{X} = \{x^0, x^1, \dots, x^p\}$, poised in the minimum Frobenius norm sense, is moreover Λ -poised in B in the minimum Frobenius norm sense provided*

$$\Lambda \geq \max_{0,1,\dots,p} \max_{x \in B} |\ell_i(x)|.$$

Critical to our development of error bounds, we state the following results.

Theorem 3. *Let $\Lambda > 0$, and let $\mathcal{X} = \{x^0, x^1, \dots, x^p\}$ be a given set of interpolation points. Let $\mathcal{B}(x^0, \Delta) \subset \mathcal{R}^d$ be a ball sufficiently large such that $\mathcal{X} \subset \mathcal{B}(x^0, \Delta)$. Suppose Assumption 1 holds with constant $L_{\nabla f}$. Define the matrix*

$$\hat{L} = \frac{1}{\Delta} \begin{bmatrix} x^1 - x^0 & x^2 - x^0 & \dots & x^p - x^0 \end{bmatrix}^\top$$

and denote its pseudoinverse via $\hat{L}^\dagger = (\hat{L}^\top \hat{L})^{-1} \hat{L}^\top$. Define

$$\epsilon_{\max} = \max_{i=1,2,\dots,p} |\tilde{f}(x^i) - f(x^i)| \quad \text{and} \quad \epsilon_0 = |\tilde{f}(x^0) - f(x^0)|.$$

If \mathcal{X} is Λ -poised in $\mathcal{B}(x^0, \Delta)$ in the minimum Frobenius norm sense, then the minimum Frobenius norm model $m(x)$ satisfies

$$\|\nabla f(x) - \nabla m(x)\| \leq \sqrt{p+1} \|\hat{L}^\dagger\| \left[(L_{\nabla f} + \|\nabla^2 m(x^0)\|) \Delta + \frac{\epsilon_0 + \epsilon_{\max}}{\Delta} \right] \quad \forall x \in \mathcal{B}(x^0, \Delta).$$

Proof. Proof. For ease of notation, we denote the quadratic underdetermined interpolation model $m(x)$ as

$$m(x) = c + g^\top x + \frac{1}{2} x^\top H x.$$

In other words, we have simply reorganized the terms in eq. (8). For an arbitrary point $x \in \mathcal{B}(x^0, \Delta)$, denote the function value error (e^f) and the gradient value error (e^g) via

$$m(x) = f(x) + e^f(x) \quad \text{and} \quad \nabla m(x) = Hx + g = \nabla f(x) + e^g(x).$$

Because $m(x)$ interpolates $\tilde{f}(x)$ at each point in \mathcal{X} , we conclude from the expression for e^f that, for each $i = 0, 1, \dots, p$,

$$\begin{aligned} m(x^i) &= \tilde{f}(x^i) && \iff \\ c + g^\top x^i + \frac{1}{2} x^{i\top} H x^i &= \tilde{f}(x^i) && \iff \\ c + g^\top x^i + \frac{1}{2} x^{i\top} H x^i - m(x) &= \tilde{f}(x^i) - m(x) && \iff \\ (x^i - x)^\top g + \frac{1}{2} (x^i - x)^\top H (x^i - x) + (x^i - x)^\top H x &= \tilde{f}(x^i) - f(x) - e^f(x). \end{aligned}$$

Now, substituting in the expression for e^g , we have for each $i = 0, 1, \dots, p$

$$(x^i - x)^\top (e^g(x) + \nabla f(x)) + \frac{1}{2} (x^i - x)^\top H (x^i - x) = \tilde{f}(x^i) - f(x) - e^f(x).$$

Trivially, we also have

$$(x^i - x)^\top (e^g(x) + \nabla f(x)) + \frac{1}{2} (x^i - x)^\top H (x^i - x) = \tilde{f}(x^i) - f(x) - e^f(x) + f(x^i) - f(x^i).$$

By Taylor's theorem and the definition of Δ , $f(x) + \nabla f(x)^\top (x^i - x) - f(x^i) \in \mathcal{O}(\Delta^2)$. Thus there exists $c_i \in \mathcal{R}$ independent of Δ such that, for all $i = 0, 1, \dots, p$,

$$(x^i - x)^\top e^g(x) + \frac{1}{2} (x^i - x)^\top H (x^i - x) = c_i \Delta^2 - e^f(x) + \tilde{f}(x^i) - f(x^i). \quad (14)$$

Now, subtracting eq. (14) for $i = 0$ from each of eq. (14) for $i = 1, \dots, p$, we get for $i = 1, \dots, p$ that

$$(x^i - x^0)^\top e^g(x) + \frac{1}{2} (x^i - x)^\top H (x^i - x) - \frac{1}{2} (x^0 - x)^\top H (x^0 - x) = (c_i - c_0) \Delta^2 + \tilde{f}(x^i) - f(x^i) - \tilde{f}(x^0) + f(x^0).$$

It now follows from the assumptions on f and \tilde{f} and the definitions of Δ , \hat{L}^\dagger , ϵ_{\max} and ϵ_0 that

$$\|e^g(x)\| \leq \sqrt{p+1} \|\hat{L}^\dagger\| \left[(L_{\nabla f} + \|H\|) \Delta + \left(\frac{\epsilon_0 + \epsilon_{\max}}{\Delta} \right) \right].$$

□

□

In order to extract a meaningful bound from [Theorem 3](#), it remains to bound both the quantities $\|\hat{L}^\dagger\|$ and $\|\nabla^2 m(x^0)\|$ appearing in [Theorem 3](#). The former quantity can be bounded by observations made in the development of Conn et al. [24][Section 5.3]. The proof of these observations involves an alternative characterization of [Definition 5](#) that we will not provide in this manuscript for the sake of concise exposition; see Conn et al. [24][Section 5.3] for full details. We state this bound on $\|\hat{L}^\dagger\|$ in [Proposition 1](#). The quantity $\|\nabla^2 m(x^0)\|$ can be bounded by mimicking the proof of a result in Conn et al. [24][Theorem 5.7]. We state and prove that bound in [Theorem 4](#).

Proposition 1. *Let \mathcal{X} be Λ -poised in the minimum Frobenius norm sense. Let [Assumption 1](#) hold. Then, \hat{L}^\dagger in the statement of [Theorem 3](#) automatically satisfies*

$$\|\hat{L}^\dagger\| \leq \sqrt{p+1} \Lambda.$$

Theorem 4. Let $\Lambda > 0$, and let $\mathcal{X} = \{x^0, x^1, \dots, x^p\}$ be a given set of interpolation points. Denote the absolute error in function value at each interpolation point by $\epsilon_i = |e(x^i, \xi_i)|$. Let $\mathcal{B}(x^0, \Delta) \subset \mathcal{R}^d$ be a ball sufficiently large such that $\mathcal{X} \subset \mathcal{B}(x^0, \Delta)$. Suppose f is continuously differentiable in an open set Ω such that $\mathcal{B}(x^0, \Delta) \subset \Omega$, and suppose ∇f is Lipschitz continuous in Ω with constant $L_{\nabla f}$. Then,

$$\|\nabla^2 m(x^0)\| \leq \frac{4(p+1)\Lambda L_{\nabla f} \sqrt{(d+1)(d+2)}}{\nu(\Delta)} + \frac{8\Lambda \sqrt{(d+1)(d+2)}}{\Delta^2 \nu(\Delta)} \sum_{i=0}^p \epsilon_i, \quad (15)$$

where we have denoted

$$\nu(\Delta) = \min \left\{ 1, \frac{1}{\Delta}, \frac{1}{\Delta^2} \right\}. \quad (16)$$

Proof. Proof. Much of the proof of Conn et al. [24][Theorem 5.7] holds here. In particular,

$$\|\nabla^2 \ell_i(x)\| \leq \frac{8\Lambda \sqrt{(d+1)(d+2)}}{\Delta^2 \nu(\Delta)}$$

holds for each $\ell_i(x)$, because it is only a property of minimum Frobenius norm Lagrange polynomials and is independent of any assumptions on noise.

As in the proof of Conn et al. [24][Theorem 5.7], we can assume without loss of generality that $f(x^0) = 0$ and that $\nabla f(x^0) = 0$ by subtracting an appropriate linear polynomial from f . If we subtract the same linear polynomial from the minimum Frobenius norm model $m(x)$, then the model Hessian $\|\nabla^2 m(x)\|$ remains unchanged.

By our subtraction of the linear polynomial, we have from Taylor's theorem that

$$\max_{x \in \mathcal{B}(x^0, \Delta)} |f(x)| \leq \frac{L_{\nabla f}}{2} \Delta^2.$$

Thus, by eq. (13),

$$\begin{aligned} \|\nabla^2 m(x^0)\| &\leq \sum_{i=0}^p |\tilde{f}(x^i)| \|\nabla^2 \ell_i(x)\| \leq \sum_{i=0}^p (|f(x^i)| + \epsilon_i) \|\nabla^2 \ell_i(x)\| \\ &\leq \sum_{i=0}^p \left[\frac{4\Lambda L_{\nabla f} \sqrt{(d+1)(d+2)}}{\nu(\Delta)} + \frac{8\Lambda \sqrt{(d+1)(d+2)} \epsilon_i}{\Delta^2 \nu(\Delta)} \right], \end{aligned}$$

as we meant to show. \square \square

Theorem 4 establishes that the norm of the model Hessian is upper bounded, either deterministically or with high probability, when \tilde{f} is a zeroth-order oracle as defined in [Definition 1](#). [Theorem 3](#), [Proposition 1](#), and [Theorem 4](#) taken together motivate two algorithmic features that we now discuss.

3.1.1 Decoupling the Sampling Radius from the Trust Region Radius

Combining the results in [Theorem 3](#), [Proposition 1](#), and [Theorem 4](#), we see that a bound on $\|\nabla f(x) - \nabla m(x)\|$ is minimized (as a function of Δ) provided

$$\Delta = \min \left\{ \sqrt{\frac{\epsilon_0 + \epsilon_{\max} + 8\Lambda \sqrt{(d+1)(d+2)} \sum_{i=0}^p \epsilon_i}{L_{\nabla f} (1 + 4(p+1) \sqrt{(d+1)(d+2)})}}, 1 \right\}.$$

If we make the coarse assumption that each ϵ term ($\epsilon_i, \epsilon_0, \epsilon_{\max}$) is bounded by $\mu\epsilon_f$ for some small multiple $\mu \geq 1$ (for example, this is true with $\mu = 1$ by definition in the deterministically bounded noise regime), then we can simplify this result to

$$\Delta \approx \min \left\{ \sqrt{\frac{2 + 8\Lambda(p+1)\sqrt{(d+1)(d+2)}}{1 + 4(p+1)\sqrt{(d+1)(d+2)}}} \sqrt{\frac{\mu\epsilon_f}{L_{\nabla f}}}, 1 \right\}.$$

Moreover, assuming $\Lambda \approx 1$ (which we discuss more in the next subsection), this greatly simplifies to

$$\Delta \approx \sqrt{\frac{2\mu\epsilon_f}{L_{\nabla f}}},$$

which is generally less than 1, since we expect ϵ_f to be small relative to $L_{\nabla f}$. Motivated by this observation, our algorithm explicitly decouples the trust-region radius from the sampling radius. Our algorithm maintains running estimates, $\tilde{\epsilon}_f$ and $\tilde{L}_{\nabla f}$, of ϵ_f and $L_{\nabla f}$, respectively. Given parameters $\mu \geq 1$ and $\bar{\Lambda} \geq 1$, if the current trust region is $\mathcal{B}(x^k, \Delta_k)$, then our algorithm will ensure that a set of interpolation points \mathcal{X} is $\bar{\Lambda}$ -poised on the set $\mathcal{B}(x^k, \max\{\Delta_k, \sqrt{2\mu\tilde{\epsilon}_f/\tilde{L}_{\nabla f}}\})$. This is a departure from standard model-based methods.

3.1.2 Careful Maintenance of Poisedness

Combining the results in [Theorem 3](#), [Proposition 1](#), and [Theorem 4](#), we see that the first-order error made by a minimum Frobenius norm model on a ball of radius Δ , with a set of interpolation points that are Λ -poised on that ball, scales quadratically with Λ in the worst case. Thus, when selecting a set \mathcal{X} of interpolation points, we intend to keep Λ bounded. This is achievable by employing an analog of Conn et al. [24][Algorithm 6.3], which we state in [Algorithm 2](#).

It is proven in Conn et al. [24][Theorem 6.6] that [Algorithm 2](#) terminates finitely, provided one solves the trust-region subproblems in [Line 3](#) with sufficient accuracy to be able to properly evaluate the condition in [Line 4](#). We also highlight that [Algorithm 2](#) requires the initial \mathcal{X} to be poised in the minimum Frobenius norm sense. This condition is easily tested; if \mathcal{X} is not poised in the minimum Frobenius norm sense, then the inversion of $W_{\mathcal{X}}$ in (12) required in [Line 2](#) will fail. In the rare event that $W_{\mathcal{X}}$ becomes singular to working precision, our optimization method will employ an existing routine found in POUNDers [38] to select a set of d points from the history of all previously evaluated points such that (1) the set of d points taken together with x^0 form an affinely independent set and (2) $\|d - x^0\|$ is bounded by a small multiple of Δ . We then replace \mathcal{X} with this set of $d + 1$ many points. This algorithm is provided in [Algorithm 4](#).

We remark that Powell [39] is entirely dedicated to suggestions for developing a method similar to [Algorithm 2](#) that is far more efficient, in particular avoiding the solution to $\mathcal{O}(p)$ many trust-region subproblems in [Line 3](#) and moreover avoiding explicit storage and inversions of $W_{\mathcal{X}}$ in [Line 2](#) by employing low-rank updates. Implementing Powell's suggestions is an avenue for future code development that we intend to pursue. However, to be absolutely consistent with the theory in this paper, we effectively produced a direct implementation of [Algorithm 2](#). This renders the per-iteration linear algebra cost of our method very high compared with standard implementations of

Algorithm 2: Improving poisedness of \mathcal{X}

Input: Desired upper bound on poisedness $\bar{\Lambda} > 1$, initial set of points $\mathcal{X} = \{x^0, x^1, \dots, x^p\}$ poised in the minimum Frobenius norm sense, radius Δ .

- 1 **for** $k = 1, 2, \dots$ **do**
- 2 Obtain minimum Frobenius norm Lagrange polynomials for \mathcal{X} , $\{\ell_i(x) : i = 0, 1, \dots, p\}$.
- 3 Compute
$$\Lambda_{k-1} = \max_{i=0,1,\dots,p} \max_{x \in \mathcal{B}(x^0, \Delta)} |\ell_i(x)|.$$
- 4 **if** $\Lambda_{k-1} > \bar{\Lambda}$ **then**
- 5 $i_k \leftarrow \arg \max_{i=0,1,\dots,p} \max_{x \in \mathcal{B}(x^0, \Delta)} |\ell_i(x)|$
- 6 $x^+ \leftarrow \arg \max_{x \in \mathcal{B}(x^0, \Delta)} |\ell_{i_k}(x)|$
- 7 $\mathcal{X} \leftarrow \mathcal{X} \cup \{x^+\} \setminus \{x^{i_k}\}$
- 8 **else**
- 9 **Return** \mathcal{X} , a $\bar{\Lambda}$ -poised set.

model-based optimization methods. However, the metric we are concerned with in this paper is limiting the number of oracle calls, not per-iteration linear algebra costs, appropriate for real-world situations where oracle calls are computationally expensive.

3.2 Statement of DFO Algorithm

We now explicitly provide an algorithm in the framework of [Algorithm 1](#) appropriate for expensive derivative-free optimization. This algorithm is provided in [Algorithm 3](#).

[Algorithm 3](#) uses \mathcal{X} , free of any subscript notation, to denote an interpolation set; this is intended to remind the reader that we will reuse previously evaluated points as much as reasonably possible, and so \mathcal{X} generally transcends the iteration count. In every iteration $k \in \{0, 1, \dots\}$, we first obtain a noise estimate $\tilde{\epsilon}_f$ and a local gradient Lipschitz constant estimate $\tilde{L}_{\nabla f}$; we leave the means to compute these estimates intentionally vague in [Algorithm 3](#), but in [Section 5](#) we discuss how one can do this in practice. While [Algorithm 3](#) employs the same trust-region mechanism with trust-region radius Δ_k as in [Algorithm 1](#), [Algorithm 3](#) explicitly decouples Δ_k from a *sampling radius* $\bar{\Delta}_k \geq \sqrt{r\tilde{\epsilon}_f/\tilde{L}_{\nabla f}}$ for some tolerance parameter $r \geq 2$. This decoupling is done in order to optimize the accuracy of the model gradient, a principle elucidated in [Section 3.1.1](#). We then update \mathcal{X} by removing from \mathcal{X} any point x satisfying $\|x - \theta_k\| > c_s \bar{\Delta}_k$, for some parameter $c_s > 1$, to yield the interpolation set $\mathcal{X} = \{x^0 = \theta_k, x^1, \dots, x^p\}$. As described in [Section 3.1](#), the cardinality of the interpolation set must satisfy $|\mathcal{X}| \in [d + 1, (d + 1)(d + 2)/2]$. When $|\mathcal{X}| > (d + 1)(d + 2)/2$, we must remove superfluous interpolation points; we elect to remove the $|\mathcal{X}| - (d + 1)(d + 2)/2$ oldest points—oldest referring to the history of when points were added to \mathcal{X} —from \mathcal{X} . Let $\mathcal{X} - \theta_k := \begin{bmatrix} x^1 - \theta_k & \dots & x^q - \theta_k \end{bmatrix}$, the matrix of displacements of each interpolation point from

θ_k , omitting the zero column resulting from $x^0 = \theta_k$. If $\mathcal{X} - \theta_k$ is not full-rank, then we augment \mathcal{X} to contain an affinely independent set of points using [Algorithm 4](#). We then call [Algorithm 2](#) to ensure that \mathcal{X} is $\bar{\Lambda}$ -poised in $\mathcal{B}(\theta_k, \bar{\Delta}_k)$ in the minimum Frobenius norm sense.

After constructing \mathcal{X} , $\tilde{f}(x)$ is evaluated at any $x \in \mathcal{X}$ at which \tilde{f} was not previously evaluated. Then, we solve [eq. \(11\)](#) (via [eq. \(12\)](#)) and use the obtained α, β to construct a local quadratic model

$$m_k(s) = \tilde{f}(\theta_k) + g_k^T s + s^T H_k s. \quad (17)$$

The trust-region subproblem $\{\min m_k(s) : s \in \mathcal{B}(0, \Delta_k)\}$ is then solved accurately enough that the step s_k satisfies the same Cauchy decrease condition [eq. \(6\)](#) as in [Algorithm 1](#). We remark that attaining [eq. \(6\)](#) is trivial in practice, since when $\kappa_{\text{fed}} = 1$, the Cauchy step will suffice. We then evaluate \tilde{f} at the test point $\theta_k + s_k$ and augment \mathcal{X} with the test point.

Next, we compute ρ_k defined as in [eq. \(18\)](#). We highlight that [eq. \(18\)](#) (and [eq. \(7\)](#) in [Algorithm 1](#)) is different from the ratio of actual decrease to predicted decrease employed in classical trust-region methods; in particular there is an additional factor of ϵ_f in the numerator of [eq. \(18\)](#). The *relaxed ratio* [eq. \(18\)](#) was proposed to account for the noise in $\tilde{f}(\theta_k)$ and $\tilde{f}(\theta_k + s_k)$ so that the numerator is not dominated by noise when Δ_k is small. A similar strategy was also considered by Sun and Nocedal [[33](#)], except they chose to add an ϵ term to both the numerator and denominator.

The criteria to determine whether the test point is accepted or not and the rule of updating Δ_k are presented between [line 15](#) and [line 17](#). It is unchanged from [Algorithm 1](#) in Cao et al. [[34](#)].

Algorithm 3: Novel noise-aware model-based trust-region Algorithm

Input: starting point $\theta_0 \in \mathcal{R}^d$; initial trust-region radius $\Delta_0 > 0$; upper bound on trust-region radius $\Delta_{\max} \geq \Delta_0$; trust-region parameters, $\eta_1, \eta_2, \gamma \in (0, 1)$; tolerance parameter $r \geq 2$; initial interpolation set $\mathcal{X} \supseteq \{x^0 = \theta_0\}$; sampling constant $c_s > 1$; maximum poisedness constant $\bar{\Lambda}$.

1 **for** $k = 0, 1, 2, \dots$ **do**

2 Obtain noise estimate $\tilde{\epsilon}_f$ and local gradient Lipschitz constant estimate $\tilde{L}_{\nabla f}$. Ensure $\tilde{L}_{\nabla f}$ chosen large enough so that $\tilde{L}_{\nabla f} \geq r\tilde{\epsilon}_f$.

3 $\bar{\Delta}_k \leftarrow \max \left\{ \Delta_k, \sqrt{\frac{r\tilde{\epsilon}_f}{\tilde{L}_{\nabla f}}} \right\}$.

4 Remove from \mathcal{X} any point x satisfying $\|x - \theta_k\| > c_s \bar{\Delta}_k$.

5 **if** $|\mathcal{X}| > (d+1)(d+2)/2$ **then**

6 Remove the $|\mathcal{X}| - (d+1)(d+2)/2$ oldest obtained points from \mathcal{X} .

7 **if** $\text{rank}(\mathcal{X} - \theta_k) < d$ **then**

8 Augment \mathcal{X} to contain an affinely independent set of points using [Algorithm 4](#).

9 Call [Algorithm 2](#) with $\bar{\Lambda}$, \mathcal{X} , and $\bar{\Delta}_k$ to obtain new \mathcal{X} .

10 Obtain evaluations $\tilde{f}(x)$ at any $x \in \mathcal{X}$ for which we have no evaluation.

11 Solve [eq. \(11\)](#) with \mathcal{X} to obtain α, β , and construct local model [eq. \(17\)](#).

12 Compute s_k as an approximate minimizer of $\{\min m_k(s) : s \in \mathcal{B}(0, \Delta_k)\}$ such that s_k satisfies [eq. \(6\)](#).

13 Evaluate $\tilde{f}(\theta_k + s_k)$, augment $\mathcal{X} \leftarrow \mathcal{X} \cup \{\theta_k + s_k\}$.

14 Compute

$$\rho_k = \frac{\tilde{f}(\theta_k) - \tilde{f}(\theta_k + s_k) + r\tilde{\epsilon}_f}{m_k(0) - m_k(s_k)} \quad (18)$$

15 **if** $\rho_k \geq \eta_1$ **then**

$$\text{Set } \theta_{k+1} = \theta_k + s_k \text{ and } \Delta_{k+1} = \begin{cases} \min\{\gamma^{-1}\Delta_k, \Delta_{\max}\} & \text{if } \|g_k\| \geq \eta_2\Delta_k \\ \gamma\Delta_k, & \text{if } \|g_k\| < \eta_2\Delta_k \end{cases}$$

16 **else**

17 Set $\theta_{k+1} = \theta_k$ and $\Delta_{k+1} = \gamma\Delta_k$.

4 Theoretical Results

We first demonstrate that, as we intended, the model gradient of a minimum Frobenius norm quadratic model is a first-order oracle for [Type 1](#) error.

Lemma 1. *Suppose \tilde{f} is a zeroth-order oracle of [Type 1](#) for f with constant ϵ_f . In [Algorithm 3](#),*

suppose $\tilde{\epsilon}_f$ is known exactly in every iteration; that is, $\tilde{\epsilon} = \epsilon_f$. Additionally, suppose $\tilde{L}_{\nabla f}$ is a valid Lipschitz constant for ∇f on any given trust region $\mathcal{B}(\theta_k, \Delta_k)$. Denote the upper bound in eq. (15) by κ_{bmh} . Then there exists $A, B > 0$ such that the model gradient g_k is a first-order oracle for $\nabla f(\theta_k)$ with

$$\begin{aligned} p_1 &= 1, \quad \kappa_{eg} = (p+1)\bar{\Lambda}(L_{\nabla f} + \max\{A, B\epsilon_f\}), \\ \epsilon_g &= (p+1)\bar{\Lambda} \max \left\{ (L_{\nabla f} + A)\sqrt{\frac{r\epsilon_f}{L_{\nabla f}}} + (B+2)\sqrt{\frac{L_{\nabla f}\epsilon_f}{r}}, A\Delta_{\max}^3 + 2\sqrt{\frac{L_{\nabla f}\epsilon_f}{r}} \right\} \end{aligned} \quad (19)$$

Proof. Proof. Combining [Theorem 3](#), [Proposition 1](#), and [Theorem 4](#), we have that, on any iteration k of [Algorithm 3](#), the model gradient g_k satisfies

$$\|\nabla f(\theta_k) - g_k\| \leq (p+1)\bar{\Lambda} \left[(L_{\nabla f} + \|H_k\|)\bar{\Delta}_k + \frac{2\epsilon_f}{\bar{\Delta}_k} \right], \quad (20)$$

where, because we are in the deterministically bounded regime and $\mathcal{X} \in \mathcal{B}(\theta_k, \bar{\Delta}_k)$, we have from [eq. \(15\)](#) that

$$\|H_k\| \leq \frac{A}{\nu(\bar{\Delta}_k)} + \frac{B}{\bar{\Delta}_k^2 \nu(\bar{\Delta}_k)} \epsilon_f, \quad A := 4(p+1)\bar{\Lambda}L_{\nabla f}\sqrt{(d+1)(d+2)}, \quad B := 8(p+1)\bar{\Lambda}\sqrt{(d+1)(d+2)}, \quad (21)$$

for $\nu(\cdot)$ defined in [Equation \(16\)](#). We proceed in three cases.

Case 1: Suppose $\bar{\Delta}_k = \Delta_k$ and $\Delta_k \leq 1$. Note that this implies $\bar{\Delta}_k \geq \sqrt{\frac{r\epsilon_f}{L_{\nabla f}}}$, and so $\bar{\Delta}_k^{-1} \leq \sqrt{\frac{L_{\nabla f}}{r\epsilon_f}}$. Making use of this fact, we have

$$\begin{aligned} \|\nabla f(\theta_k) - g_k\| &\leq (p+1)\bar{\Lambda} \left[(L_{\nabla f} + A)\Delta_k + \frac{(B+2)\epsilon_f}{\Delta_k} \right] \\ &\leq (p+1)\bar{\Lambda} \left[(L_{\nabla f} + A)\Delta_k + (B+2)\sqrt{\frac{L_{\nabla f}\epsilon_f}{r}} \right]. \end{aligned}$$

Case 2: Suppose $\bar{\Delta}_k = \Delta_k$ and $\Delta_k > 1$. Recall the algorithmic parameter Δ_{\max} , which enforces $\Delta_k \leq \Delta_{\max}$ for all k . Then,

$$\begin{aligned} \|\nabla f(\theta_k) - g_k\| &\leq (p+1)\bar{\Lambda} \left[(L_{\nabla f} + A\Delta_k^2 + B\epsilon_f)\Delta_k + \frac{2\epsilon_f}{\Delta_k} \right] \\ &\leq (p+1)\bar{\Lambda} \left[(L_{\nabla f} + B\epsilon_f)\Delta_k + A\Delta_{\max}^3 + \frac{2\epsilon_f}{\Delta_k} \right] \\ &\leq (p+1)\bar{\Lambda} \left[(L_{\nabla f} + B\epsilon_f)\Delta_k + A\Delta_{\max}^3 + 2\sqrt{\frac{L_{\nabla f}\epsilon_f}{r}} \right]. \end{aligned}$$

Case 3: Suppose $\bar{\Delta}_k = \sqrt{\frac{r\epsilon_f}{L_{\nabla f}}}$. Recall that [Algorithm 3](#) chooses a Lipschitz constant $L_{\nabla f}$ sufficiently large such that $\bar{\Delta}_k \leq 1$ in this case. Then

$$\begin{aligned} \|\nabla f(\theta_k) - g_k\| &\leq (p+1)\bar{\Lambda} \left[(L_{\nabla f} + A + \frac{B\epsilon_f}{\bar{\Delta}_k^2})\bar{\Delta}_k + \frac{2\epsilon_f}{\bar{\Delta}_k} \right] \\ &= (p+1)\bar{\Lambda} \left[(L_{\nabla f} + A)\bar{\Delta}_k + \frac{B+2}{\bar{\Delta}_k}\epsilon_f \right] \\ &= (p+1)\bar{\Lambda} \left[(L_{\nabla f} + A)\sqrt{\frac{r\epsilon_f}{L_{\nabla f}}} + (B+2)\sqrt{\frac{L_{\nabla f}\epsilon_f}{r}} \right]. \end{aligned}$$

The desired result is therefore satisfied with the parameters defined in [eq. \(19\)](#). □ □

As a brief remark, we note from the analysis in [Lemma 1](#) that the maximum in the ϵ_g term involving the unappealing Δ_{\max}^3 term is realized only on iterations in which $\Delta_k > 1$. In fact, Δ_{\max} can be replaced with Δ_k on such iterations. The use of Δ_{\max} in this analysis is pessimistic but was chosen to make clear how ϵ_g can be derived as a quantity independent of Δ_k , as is required for the definition of a first-order oracle. The next lemma shows that the model gradient of a minimum Frobenius norm quadratic model is also a first-order oracle for [Type 2](#) error.

Lemma 2. *Suppose \tilde{f} is a zeroth-order oracle for f of [Type 2](#) with constants c and ϵ_f . Let $\bar{L}_{\nabla f}$, $\tilde{\epsilon}_f$ and κ_{bmh} be as in [Lemma 1](#). Then there exist $\mu > 1$ and $A, B > 0$ such that the model gradient g_k is a first-order oracle for $\nabla f(\theta_k)$ with*

$$\begin{aligned} p_2 &= 1 - 2(p+1)\exp(c(1-\mu)\epsilon_f), \quad \kappa_{eg} = (p+1)\bar{\Lambda}(L_{\nabla f} + \max\{A, B\mu\epsilon_f\}) \\ \epsilon_g &= (p+1)\bar{\Lambda} \max \left\{ (L_{\nabla f} + A)\sqrt{\frac{r\epsilon_f}{L_{\nabla f}}} + (B\mu + 2)\sqrt{\frac{L_{\nabla f}\epsilon_f}{r}}, A\Delta_{\max}^3 + 2\sqrt{\frac{L_{\nabla f}\epsilon_f}{r}} \right\}. \end{aligned} \quad (22)$$

Proof. Proof. By the same reasoning that led to [eq. \(20\)](#), we have that in the k th iteration of [Algorithm 3](#),

$$\|\nabla f(\theta_k) - g_k\| \leq (p+1)\bar{\Lambda} \left[(L_{\nabla f} + \|H_k\|)\bar{\Delta}_k + \frac{\epsilon_0 + \epsilon_{\max}}{\bar{\Delta}_k} \right].$$

We have only to yield a tail bound on $\epsilon_0 + \epsilon_{\max}$, which we do coarsely¹ with a union bound. That is, denoting $X_i = |e(x^i, \xi_i)|$ (recalling [eq. \(2\)](#) for the definition of $e(\theta, \xi)$) and letting ξ be a vector of realized random variables ξ_i , we have, for any $t \geq 0$,

$$\begin{aligned} \mathbb{P}_{\xi} \left[X_0 + \max_{i=1, \dots, p} X_i \geq t \right] &\leq \mathbb{P}_{\xi} [X_0 \geq \frac{t}{2}] + \mathbb{P}_{\xi} \left[\max_{i=1, \dots, p} X_i \geq \frac{t}{2} \right] \\ &\leq \exp(c(\epsilon_f - \frac{t}{2})) + \mathbb{P}_{\xi} \left[\max_{i=1, \dots, p} X_i \geq \frac{t}{2} \right] \\ &\leq \exp(c(\epsilon_f - \frac{t}{2})) + \sum_{i=1}^p \mathbb{P}_{\xi} [X_i > \frac{t}{2}] \\ &\leq (p+1)\exp(c(\epsilon_f - \frac{t}{2})). \end{aligned}$$

To work with the same quantities as employed in [Lemma 1](#), we let $\mu > 1$ denote an arbitrary multiplier and consider the special case

$$\mathbb{P}_{\xi} \left[X_0 + \max_{i=1, \dots, p} X_i \geq 2\mu\epsilon_f \right] \leq (p+1)\exp(c(1-\mu)\epsilon_f) := p_1(\mu).$$

Because we are in the independent subexponential noise regime, we this time obtain from [eq. \(15\)](#) that

$$\|H_k\| \leq \frac{4(p+1)\Lambda L_{\nabla f} \sqrt{(d+1)(d+2)}}{\nu(\bar{\Delta}_k)} + \frac{8\Lambda \sqrt{(d+1)(d+2)}}{\bar{\Delta}_k^2 \nu(\bar{\Delta}_k)} \sum_{i=0}^p X_i.$$

¹If we cast stronger assumptions about the moment-generating function of \tilde{f} , tighter bounds could be yielded via Chernoff bound arguments. To retain the same general definition of zeroth-order oracle that is stated only in terms of tail bounds, as employed in [Cao et al. \[34\]](#), we do not make such assumptions here.

Employing the same union bound argument as before,

$$\mathbb{P}_\xi \left[\sum_{i=0}^p X_i \geq t \right] \leq (p+1) \exp \left(c \left(\epsilon_f - \frac{t}{p+1} \right) \right).$$

Let $\mu > 1$ be the same arbitrary multiplier as before. To work with the same quantities employed in [Lemma 1](#), we are concerned with the tail probability

$$\mathbb{P}_\xi \left[\sum_{i=0}^p X_i \geq \mu(p+1)\epsilon_f \right] \leq (p+1) \exp(c(1-\mu)\epsilon_f) = p_1(\mu).$$

Now, we can bound

$$\|H_k\| \leq \frac{A}{\nu(\bar{\Delta}_k)} + \frac{B\mu}{\bar{\Delta}_k^2 \nu(\bar{\Delta}_k)} \epsilon_f \quad \text{with probability } p_1(\mu),$$

where A, B are the same as in [Lemma 1](#).

Proceeding in the same three cases as in [Lemma 1](#), one can almost identically conclude that, for any $\mu > 1$, g_k is a first-order oracle with probability $1 - 2p_1(\mu)$ and constants $\kappa_{eg} = (p+1)\bar{\Lambda}(L_{\nabla f} + \max\{A, B\mu\epsilon_f\})$ and $\epsilon_g = (p+1)\bar{\Lambda} \max \left\{ (L_{\nabla f} + A) \sqrt{\frac{r\epsilon_f}{L_{\nabla f}}} + (B\mu + 2) \sqrt{\frac{L_{\nabla f}\epsilon_f}{r}}, A\Delta_{\max}^3 + 2\sqrt{\frac{L_{\nabla f}\epsilon_f}{r}} \right\}$. □

We now immediately conclude the following convergence results for [Algorithm 3](#). [Theorem 5](#) and [Theorem 6](#) are direct results of [Theorem 1](#) and [Theorem 2](#), respectively, and follow when we explicitly consider how ϵ_g is a function of ϵ_f when we employ minimum Frobenius norm modeling.

Theorem 5. *Suppose [Assumption 1](#) and [2](#) hold. Suppose \tilde{f} is a zeroth-order oracle of [Type 1](#) for f with constant ϵ_f . In [Algorithm 3](#), suppose $\tilde{\epsilon}_f$ is known exactly in every iteration; that is, $\tilde{\epsilon}_f = \epsilon_f$. Additionally, suppose $\tilde{L}_{\nabla f}$ is a valid Lipschitz constant for ∇f on a given trust region $\mathcal{B}(\theta_k, \Delta_k)$. Let $\{\Theta_k\}$ denote the sequence of random variables with realizations $\{\theta_k\}$ generated by [Algorithm 3](#). There exists κ_1 , independent of ϵ_f, ϵ_g but dependent on κ_{eg}, p_1 , such that given any*

$$\epsilon > \kappa_1 \sqrt{\epsilon_f},$$

it holds that

$$\mathbb{P} \left[\min_{0 \leq k \leq T-1} \|\nabla f(\Theta_k)\| \leq \epsilon \right] \geq 1 - \exp(-\mathcal{O}(T))$$

for any $T \in \mathcal{O}\left(\frac{1}{\epsilon^2}\right)$.

Proof. Proof. This follows from [Theorem 1](#) and [Lemma 1](#) with $p_1, \kappa_{eg}, \epsilon_g$ as defined in [Lemma 1](#). □

Theorem 6. *Suppose [Assumption 1](#) and [2](#) hold. Suppose \tilde{f} is a zeroth-order oracle of [Type 2](#) for f with constant ϵ_f and c . In [Algorithm 3](#), suppose $\tilde{\epsilon}_f$ is known exactly in every iteration; that is, $\tilde{\epsilon}_f = \epsilon_f$. Additionally, suppose $\tilde{L}_{\nabla f}$ is a valid Lipschitz constant for ∇f on a given trust region*

$\mathcal{B}(\theta_k, \Delta_k)$. Let $\{\Theta_k\}$ denote the sequence of random variables with realizations $\{\theta_k\}$ generated by [Algorithm 3](#). There exists κ_2 , independent of ϵ_f, ϵ_g but dependent on κ_{eg}, p_1, c , such that given any

$$\epsilon > \kappa_2 \sqrt{\epsilon_f + 1/c},$$

it holds that

$$\mathbb{P} \left[\min_{0 \leq k \leq T-1} \|\nabla f(\Theta_k)\| \leq \epsilon \right] \geq 1 - 2 \exp(-\mathcal{O}(T)) - \exp(-ct/4)$$

for any $T \in \mathcal{O}(\frac{1}{\epsilon^2})$ and any $t > 0$.

Proof. Proof. This follows from [Theorem 2](#) and [Lemma 2](#), with p_1, κ_{eg} and ϵ_g as defined in [Lemma 2](#). □ □

5 Numerical Results

We now study the practical performance of an implementation of [Algorithm 3](#) and other methods commonly used for optimizing VQAs.

5.1 ANATRA

We have created a reasonably faithful Python implementation of [Algorithm 3](#). We refer to this implementation as ANATRA, short for A Noise-Aware Trust-Region Algorithm. ANATRA differs from [Algorithm 3](#) in a few minor ways, which we now list.

1. In [Line 9](#) we do not actually run [Algorithm 2](#) until a $\bar{\Lambda}$ -poised set is returned. Instead, if \mathcal{X} is not already $\bar{\Lambda}$ -poised, then we run a *single iteration* of [Algorithm 2](#) and return an improved, but not necessarily $\bar{\Lambda}$ -poised, interpolation set \mathcal{X} . With this modification, [Algorithm 2](#) additionally returns a validity flag that is set to True provided the set \mathcal{X} returned by [Algorithm 2](#) is indeed $\bar{\Lambda}$ -poised.
2. We do not evaluate $\tilde{f}(\theta_k + s_k)$ in [Line 13](#) unless at least one of the following two conditions holds: either the validity flag returned in [Line 9](#) is True, or the trial step satisfies $\|s_k\| \geq 0.01\Delta_k$. When $\tilde{f}(\theta_k + s_k)$ is not evaluated, we set $\Delta_{k+1} \leftarrow \Delta_k$ and $\theta_{k+1} \leftarrow \theta_k$ and return to [Line 2](#).
3. [Algorithm 1](#) was analyzed with a trust-region adjustment step like that in [Line 15](#). However, we found it more practical to use the following trust-region adjustment step instead: If $\rho_k \geq \eta_1$ and $\|s_k\| > 0.75\Delta_k$, then $\Delta_{k+1} \leftarrow \gamma^{-1}\Delta_k$. Otherwise (if $\rho_k < \eta_1$), then $\Delta_{k+1} \leftarrow \gamma\Delta_k$ only provided the validity flag is currently set to True. We remark that both this change and the previous change are also employed in POUNDers [\[38\]](#).
4. While the analysis of [Algorithm 1](#) certainly thrives on the nonmonotonicity of noisy function values, as evident in the ratio [eq. \(7\)](#), we found allowing too much nonmonotonicity can deter practical performance. In particular, we maintain a memory of the lowest noisy function

value $\tilde{f}(\theta_{best})$ observed up until iteration k (and its corresponding θ_{best}), which we will denote \tilde{f}_{best} . If, at the end of the k th iteration of [Algorithm 3](#), $\tilde{f}(\theta_k) \geq \tilde{f}_{best} + r\epsilon_f$, then we replace the incumbent θ_k with the stored θ_{best} . While this goes against the theory of [Algorithm 1](#), and hence [Algorithm 3](#), this safeguard against *too much* non-monotonicity appears to greatly aid practical performance.

In terms of parameters for [Algorithm 3](#), we use values that are considered fairly standard in model-based trust-region methods. In particular, we use $\eta_1 = 0.25$, $\gamma = 0.5$, $c_s = \sqrt{d}$, and $\bar{\Lambda} = \sqrt{d}$. We note that owing to our third adjustment above, there is no η_2 in our method. In terms of the parameter that is unique to an algorithm within the framework of [Algorithm 1](#), we set $r = 2$ in [Algorithm 3](#).

We remark that a lot of freedom exists in how [Line 1](#) is performed. In different numerical tests we will have different methods of obtaining $\tilde{\epsilon}_f$. In all of our numerical tests, however, we will always compute $\tilde{L}_{\nabla f}$ in the same way. In the first iteration ($k = 0$) of [Algorithm 3](#), we simply let $\tilde{L}_{\nabla f} = 1$. Otherwise, in any iteration where the validity flag is True at the time [Line 1](#) is reached, we update $\tilde{L}_{\nabla f}$ to be the largest eigenvalue of the most recent model Hessian H_{k-1} . Otherwise, if the validity flag is False when [Line 1](#) is reached, we do not update the estimate $\tilde{L}_{\nabla f}$.

5.2 Comparator Methods

In our tests it is naturally appropriate to compare ANATRA with the various solvers wrapped in `scikit-quant` [23]. In particular, we choose to compare ANATRA with PyBOBYQA [40], NOMAD [41], and ImFil [42], each as wrapped in `scikit-quant`. Of the four `scikit-quant` solvers discussed in Lavrijsen et al. [23], we are noticeably missing SnobFit [43]. This omission is intentional; whereas the other three solvers are local methods, SnobFit was designed for global optimization. SnobFit constructs local quadratic models of the objective function centered at points selected within a branch-and-bound framework. As such, the performance of SnobFit critically depends on the choice of a set of bound constraints. Because we are testing the performance of optimization methods for *unconstrained* problems, bound constraints were not provided to any solver. Preliminary tests indeed showed, as we expected, that the performance of SnobFit was very sensitive to the size of provided bound constraints. One should not discount the utility of SnobFit based on these tests, but a practitioner should be aware that SnobFit is only a reasonable comparator in settings where a meaningfully bounded domain can be provided by the user.

ImFil Implicit filtering [42] is a method with a fairly sophisticated implementation (which we denote `ImFil`). At its core, implicit filtering is an inexact quasi-Newton method. Gradient approximations are constructed via central finite differences with initially coarse difference parameters. On any iteration in which the center of the finite difference stencil exhibits a lower objective value than all of the forward or backward evaluation points, a *stencil failure* is declared, and the finite difference parameter is decreased. The original motivation for implicit filtering came from noisy problems; in fact, the convergence of implicit filtering to local minimizers can be established

when the objective function is the sum of a ground truth smooth function f_s and a high-frequency low-amplitude noisy function f_n provided $f_n \rightarrow 0$ at local minimizers of f_s [44]. While such an assumption may not be precisely satisfied by our problem setting, `ImFil` remains a competitive method in the presence of more general noise settings, including ours.

NOMAD `NOMAD` [41] is a widely used implementation of a mesh-adaptive direct search algorithm [45]. Unlike model-based methods (including all of the methods discussed so far), direct search methods never explicitly construct a model of a gradient or higher-order derivatives. Instead, a mesh-adaptive direct search (MADS) algorithm maintains an incumbent point and on each iteration generates a set of points on a(n implicit) mesh covering the feasible region. If sufficient objective improvement is found on a generated mesh point, the incumbent is updated. Because there is so much freedom in how points are generated on the mesh and how the mesh is updated between iterations and because any number of heuristics can be inserted into a so-called search step of MADS, implementation details of MADS algorithms are critical. While MADS algorithms, and in particular `NOMAD`, were not designed for noisy problems, an intuitive argument can be made that direct search methods could be slightly more robust to noise than are model-based methods, since they cannot be affected by poor (interpolation) models that have accumulated too many noise function evaluations. Recent work has seen extension of MADS algorithms to stochastic problems [46], but these extensions are not currently part of `NOMAD`.

PyBOBYQA `PyBOBYQA` is an extension of `BOBYQA`, a widely used model-based derivative-free solver [25]. Because `ANATRA` also belongs to the class of model-based derivative-free solvers, `PyBOBYQA` is the closest in spirit to `ANATRA` among all the comparator methods in this study. Of particular note, `PyBOBYQA` implements several heuristics designed to make `BOBYQA` more robust to noise, which is of critical importance in our setting. This robustness is accomplished primarily via a *restart* mechanism. `PyBOBYQA` stores the norm of model gradient and Hessian norms over several past iterations. If an exponentially increasing trend is detected over that short history, then the trust-region radius is increased, and several interpolation points, including the trust-region center, are selectively replaced.

SPSA In addition to the discussed solvers wrapped by `scikit-quant`, we test the method of simultaneous perturbation by stochastic approximation (SPSA) [47]. Conceptually, `SPSA` is a remarkably simple method that computes a coarse stochastic gradient approximation by computing a two-point finite-difference gradient estimate. At first blush, two-point gradient estimates are immensely attractive, because it appears that considerable optimization progress can be made even when the dimension of the problem is large; contrast these two evaluations with any model-based method that effectively requires $\mathcal{O}(d)$ many function evaluations to even begin the optimization. While asymptotic convergence to local minima can be established for `SPSA` [48, 49], various parameters, including the step-size sequence, can be difficult to tune in practice. Despite this, `SPSA` has become popular within the quantum computing community. A note on the Qiskit documentation [50]

states:

“SPSA can be used in the presence of noise, and it is therefore indicated in situations involving measurement uncertainty on a quantum computation when finding a minimum. If you are executing a variational algorithm using an OpenQASM simulator or a real device, SPSA would be the most recommended choice among the optimizers provided here.”

For these reasons, we have chosen to include Qiskit’s implementation of SPSA among the tested solvers. We note that, as with all of the solvers tested in our experiments, we only use default settings, and in particular we do not attempt to tune the learning rate of SPSA. The intention behind this choice is to provide further evidence for the well-known empirical observation that trust-region methods (such as ANATRA and PyBOBYQA) are relatively insensitive to hyperparameter selections, when compared with methods based on stochastic approximation, such as SPSA.

5.3 Tests on Synthetic Problems

We strongly believe that an important numerical test of a model-based derivative-free method in the presence of noise is arguably the simplest one imaginable: a quadratic function perturbed by additive noise. In particular, for a given dimension d so that $\theta \in \mathcal{R}^d$,

$$\tilde{f}(\theta, \xi) = \theta^\top \theta + \xi. \tag{23}$$

The objective function in eq. (23) is an ideal test function for these methods because, if there were no noise, any derivative-free method that attempts to build a quadratic interpolation model ought to construct a perfect (that is, the quadratic interpolation model exactly equals the objective function) local model of the objective function as soon as $2d + 1$ function evaluations are performed on a set of points exhibiting reasonable geometry. In our tests, in an effort to test both deterministically bounded noise regimes and independent subexponential noise regimes, we let ξ in eq. (23) be uniformly drawn at random from $[-\epsilon_f, \epsilon_f]$ or else $\xi \sim \mathcal{N}(0, \epsilon_f^2)$, respectively for a noise level ϵ_f that we choose. For the synthetic tests, we explicitly provide ANATRA with the chosen value of ϵ_f as an input. Obviously, in our real problems, we will not have this luxury, but we aim to demonstrate in the synthetic tests how well ANATRA does given idealized estimates. ANATRA and PyBOBYQA both require a construction of a local quadratic model in each iteration and therefore have relatively large per-iteration linear algebra cost as measured in CPU time compared to other solvers, especially when the dimension is large. However, the main computational cost in our problems of interest is the number of function evaluations. With this perspective, the CPU time used for model construction in both algorithms is negligible. Consequently, we present performance plots solely with respect to the number of function evaluations.

Median performance, over 30 trials for each solver, is illustrated for $d = 2$ in Figure 1 and for $d = 10$ in Figure 2. In these tests we chose θ_0 as the vector of all ones, and we test on noise levels $\epsilon_f \in \{10^{-5}, 10^{-3}, 10^{-1}\}$. In general, we observe a clear preference for ANATRA except for the lowest level of noise ($\epsilon_f = 10^{-5}$) and on the larger problem ($d = 10$), in which PyBOBYQA finds better-quality solutions within the budget of $25(d + 1)$ function evaluations. We note that the

relative preference for using PyBOBYQA decreases as the noise increases. This was to be expected, since as this paper further demonstrates, the quality of a quadratic interpolation models become proportionally poor as ϵ_f in a noise oracle increases, and the noise mitigation technique employed by PyBOBYQA is only a heuristic.

A second synthetic problem that we find important for comparing derivative-free optimization methods is the standard benchmark 2-dimensional Rosenbrock function perturbed by additive noise. That is,

$$\tilde{f}(\theta, \xi) = 100(\theta_2 - \theta_1^2)^2 + (1 - \theta_1)^2 + \xi. \quad (24)$$

The Rosenbrock function is especially good for testing the efficacy of *model-based* derivative-free methods because the Rosenbrock function is a quartic polynomial, meaning that a quadratic interpolation model will generally never be a perfect model. Moreover, the Rosenbrock function is highly nonlinear but interpretably so; any descent-seeking trajectory must turn around a curved valley, the base of which is defined by the curve $\theta_2 = \theta_1^2$. However, even as a pathologically nonlinear and nonconvex function, the 2-dimensional Rosenbrock has exactly one local (global) minimum, making benchmarking in terms of function values straightforward.

Results comparing the median performance over 30 trials of the five solvers are displayed in [Figure 3](#). In these runs we used the starting point of the origin, which is conveniently on the curve $\theta_2 = \theta_1^2$; that is, this test is designed not to test an algorithm’s ability to find the bottom of the valley but instead to test an algorithm’s ability to follow the nonlinear valley to the global minimum. We note a few behaviors that did not appear in the test with the simple quadratic functions. First, one may note that SPSA does not seem to start from the same starting point as the other solvers; the reason that because of the finite differencing scheme innate to SPSA, the initial point is never actually evaluated. Moreover, because the gradient is relatively small near $\theta_2 = \theta_1^2$ but relatively large farther away from the same curve, the gradient estimates obtained from the randomized two-point difference scheme employed by SPSA lead to a trajectory that tends to stay near the valley but never gets too close to the bottom until/unless a very small step size is employed. Of the remaining solvers, it is notable that a relative preference for NOMAD versus ImFil seems to have switched for this problem. A potential explanation for this may lie in the fact that ImFil uses a fairly rigid (coordinate-aligned) finite difference gradient estimator; this stencil centered near any point on $\theta_2 = \theta_1^2$ will not overlap well with the valley of descent. This will trigger multiple stencil failures until the stencil size is quite small, at which point finding descent is difficult in the presence of noisy evaluations. NOMAD, on the other hand, generates polling directions less rigidly on the mesh and is more likely to identify an improving point. Of particular interest to this paper, ANATRA and PyBOBYQA perform similarly on the lowest level of noise ($\epsilon_f = 10^{-5}$), but the preference for using ANATRA becomes increasingly clear as the noise increases.

5.4 Tests on VQA Problems

The synthetic tests of the preceding section were designed to establish why we believe a noise-aware model-based method like ANATRA is a good choice for noise-perturbed smooth optimization.

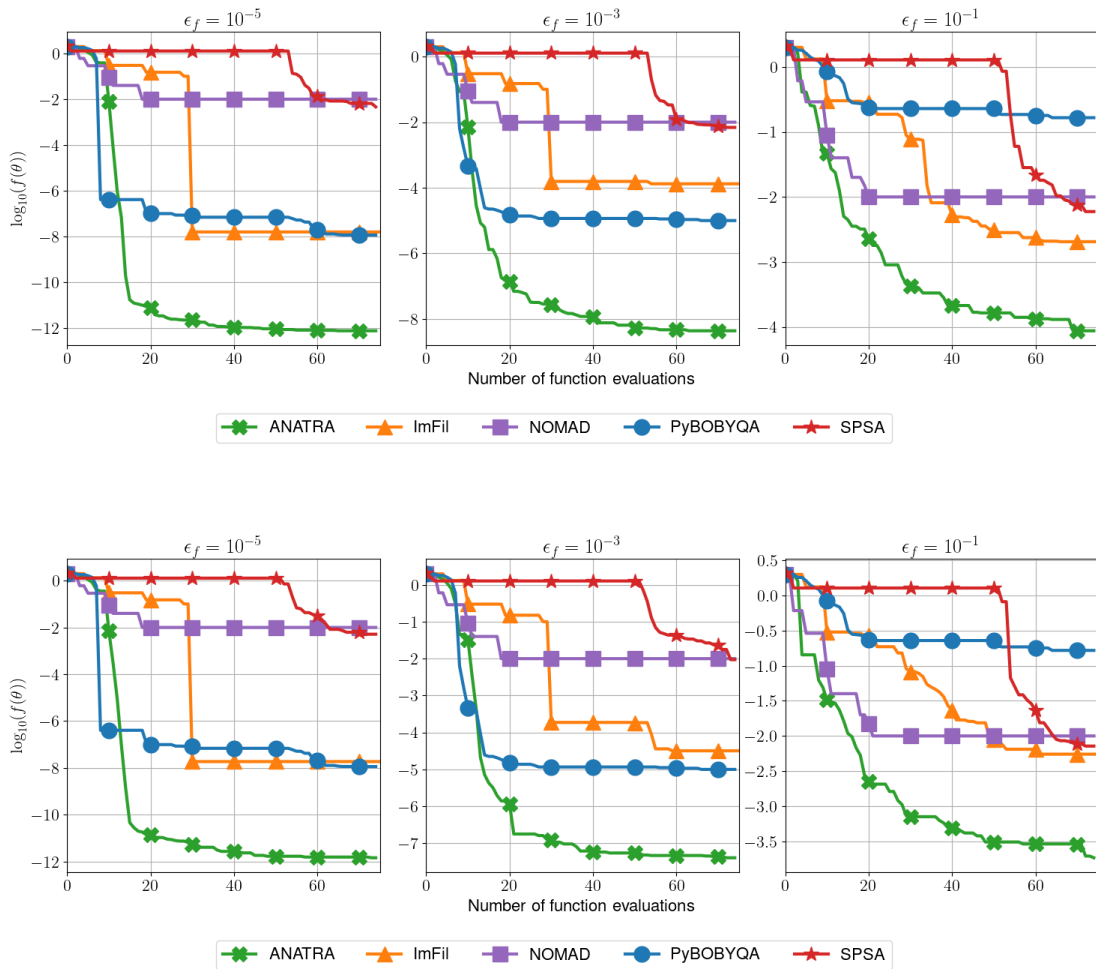


Figure 1: Results for $d = 2$ -dimensional quadratic problems eq. (23). Top row corresponds to uniform noise; bottom row corresponds to Gaussian noise. Throughout all of these plots, the solid lines correspond to the median ground truth objective value over 30 runs of the best point evaluated by the solver.

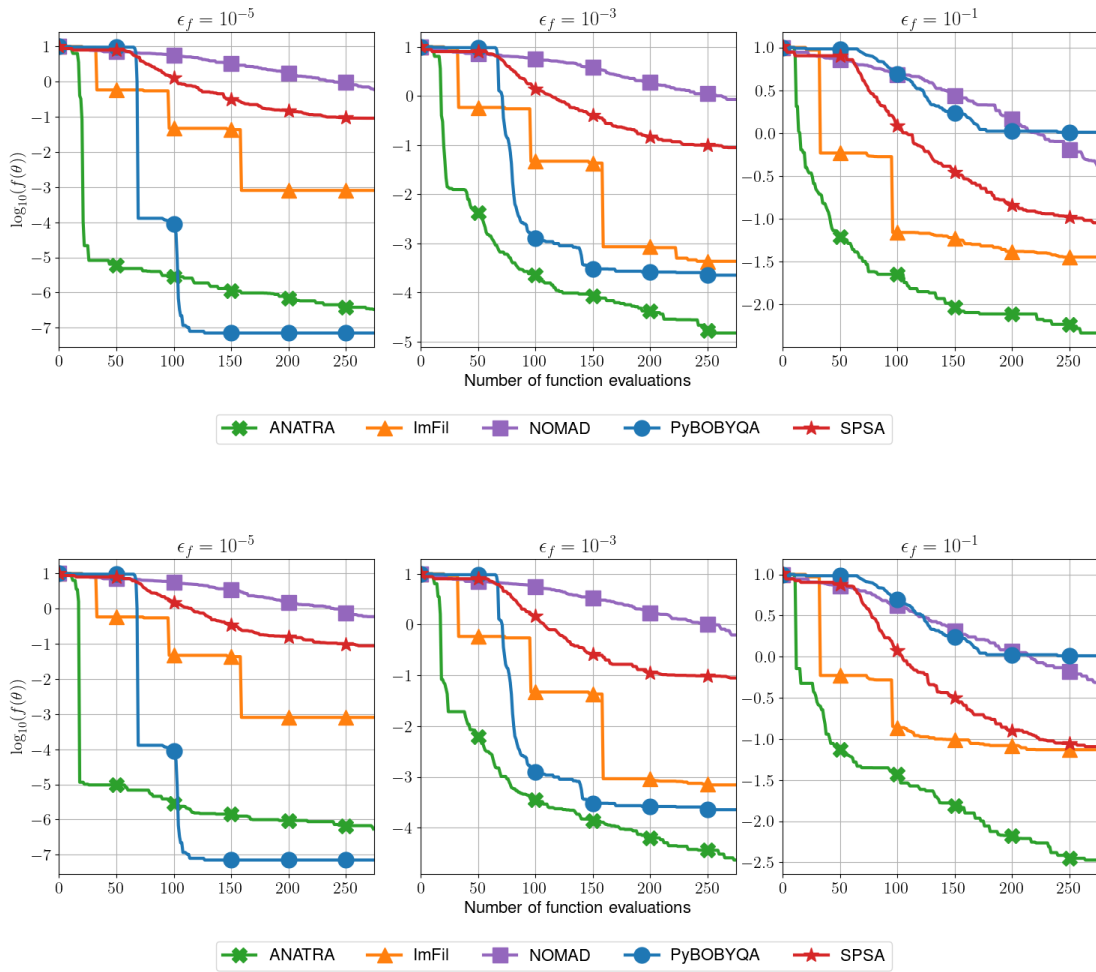


Figure 2: Same as Figure 1 but with $d = 10$ -dimensional quadratic functions.

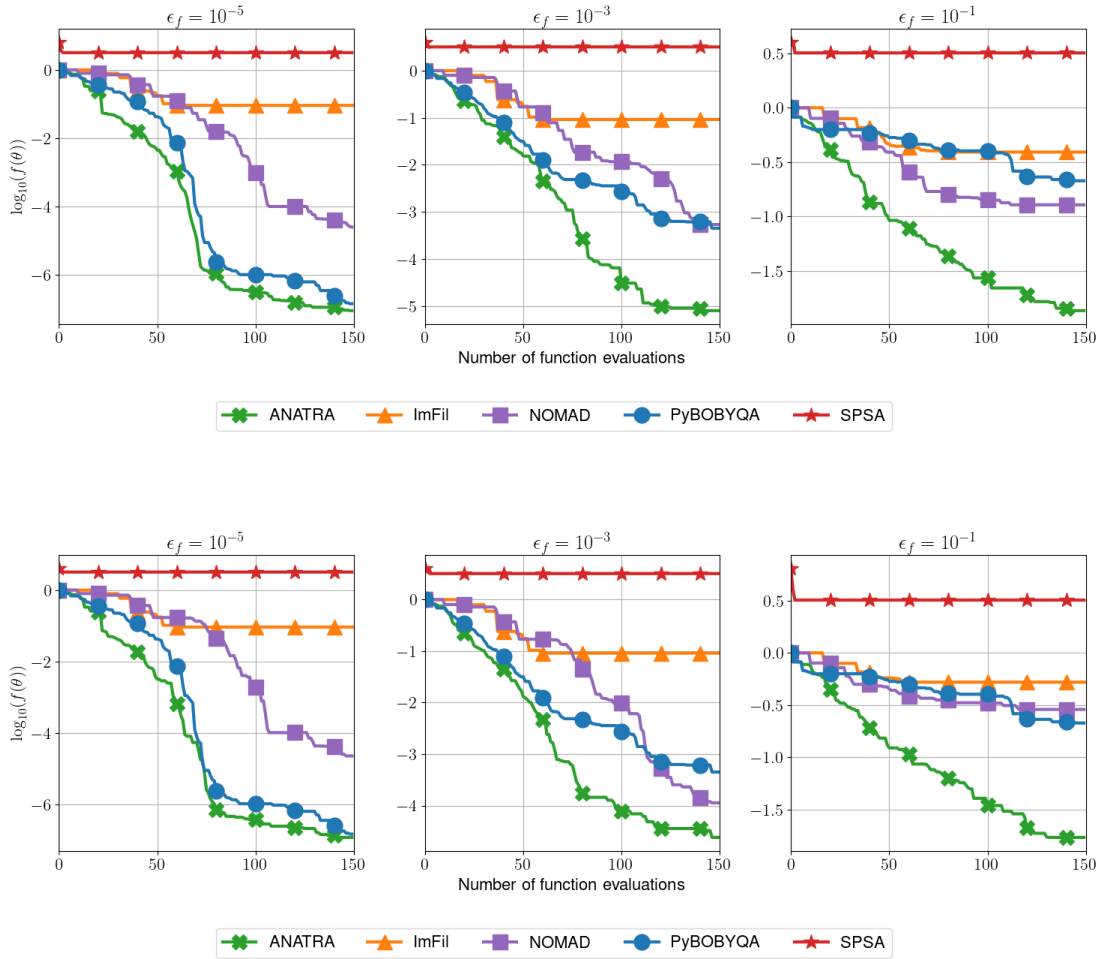


Figure 3: Comparing solvers on eq. (24). Top plots correspond to uniform noise; bottom plots correspond to Gaussian noise.

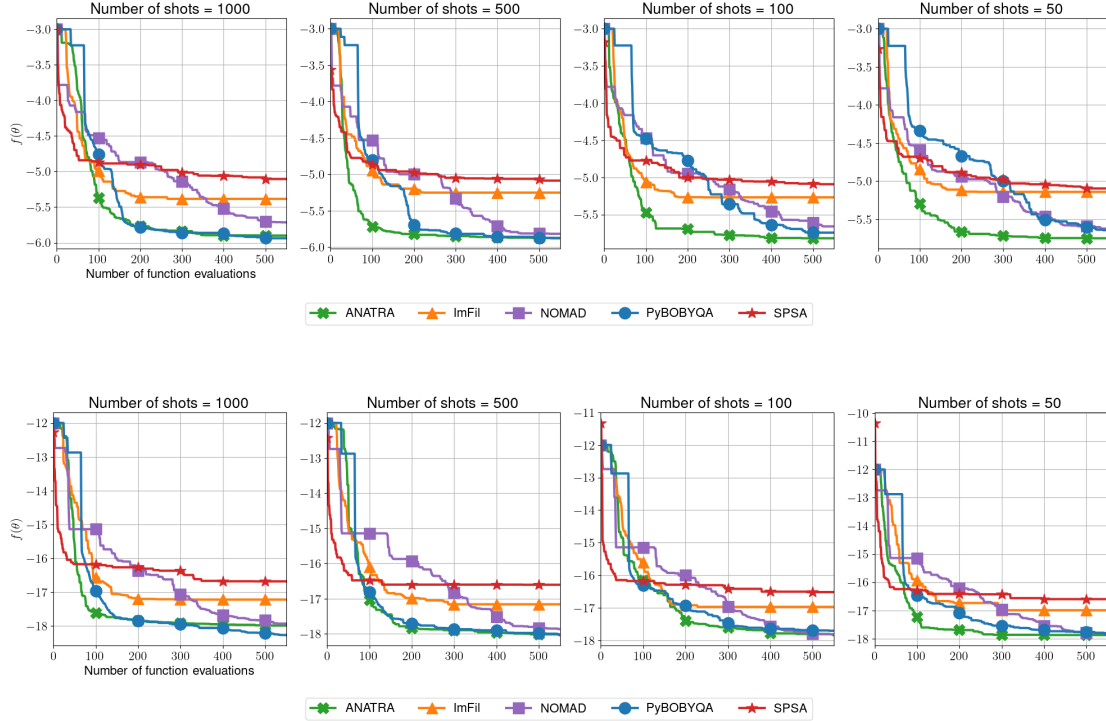


Figure 4: Comparing solvers on QAOA MaxCut problems. Top plots correspond to the toy graph, and bottom plots correspond to the Chvátal graph.

To further this claim, we now perform tests on standard QAOA benchmarks to demonstrate the performance of our solver on simulations of real problems, which is the original motivation for our work. We simulate QAOA MaxCut circuits in Qiskit [51] with a depth of five, resulting in a set of (ten) parameters. Of course, to mirror the real-world, we no longer assume that we know ϵ_f as an input to ANATRA. Instead, when we compute the sample average of the MaxCut objective values suggested by the quantum device, we additionally compute the standard error; we use the standard error as $\tilde{\epsilon}_f$. In our tests we vary the shot counts per function evaluation to be in $\{50, 100, 500, 1000\}$.

We experiment with the MaxCut problem both on a toy graph with MaxCut value of 6 and on the Chvátal graph, a standard benchmark that has a MaxCut value of 20. In our first set of QAOA experiments, illustrated in Figure 4, we employed the QASM simulator in Qiskit to simulate an ideal execution of the QAOA circuit.

The results in Figure 4 mirror most of our expectations that came from the synthetic tests. In less noisy settings (when the shot count is 1000 shots per evaluation), there is little distinction, but perhaps a slight preference, for using PyBOBYQA over ANATRA. However, as the noise increases (the shot count decreases), we see an increasingly clear preference for employing ANATRA, both in terms of final median solution quality and in terms of efficiency to reach said median solution quality.

The practical intention of ANATRA was to provide a noise-aware solver, where the source of the noise need not be purely stochastic, but rather real gate noise on near-term quantum devices. As

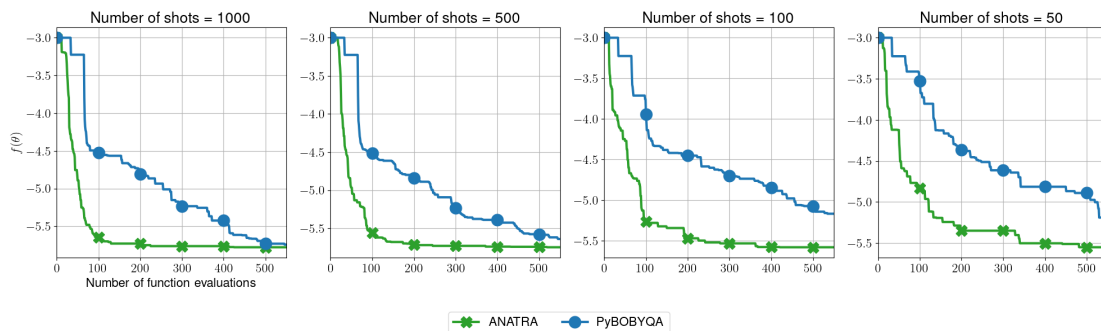


Figure 5: Comparing the performance of ANATRA and PyBOBYQA on the QAOA MaxCut problems with the toy graph, but on IBM Algiers, as opposed to an idealized QASM simulator.

such, we also experimented with ANATRA on the smaller (toy graph) QAOA MaxCut instance on IBM Algiers. Due to time and budget constraints, we only ran this second set of experiments with the two best-performing solvers from the tests illustrated in Figure 4, PyBOBYQA and ANATRA. Although not entirely technically correct, it is reasonable to continue using the standard error of cost function estimates to estimate ϵ_f in the presence of gate noise. Developing more robust means of estimating ϵ_f to better align with Definition 1 is a topic for future research. Median results are displayed in Figure 5. We comment that while both PyBOBYQA and ANATRA perform worse in this noisier environment as compared to the idealized QASM simulator, the relative advantage of using ANATRA over PyBOBYQA has clearly increased in this noisier setting.

6 Discussion

We have presented, analyzed, and tested a noise-aware model-based trust-region algorithm to solve noisy derivative-free optimization problems, a problem class that can encompass VQA. In our theory, function evaluations are assumed to be obtained from a zeroth-order oracle with deterministically bounded noise or subexponential noise. Our proposed algorithm was based on an established noise-aware trust-region method but employed algorithmic devices to carefully maintain poised-ness of interpolation points. In addition, unlike most classical model-based trust-region methods, our method decoupled the trust-region radius from the sampling radius. These two considerations were made in order to guarantee conditions concerning first-order oracles, required by the theory of the original noise-aware trust-region method, were satisfied. Building on previous results, we proved that with high probability our method exhibits a worst-case $\mathcal{O}(\epsilon^{-2})$ convergence rate to an ϵ -neighborhood of a local minima provided ϵ is greater than a function of the noise level ϵ_f . Numerical experiments demonstrate that our proposed algorithm outperforms alternative solvers, particularly in highly noisy regimes, such as when shot counts on a quantum device are low.

The work in this manuscript leaves open several avenues for future development. As mentioned, the techniques proposed in Powell [39] could alleviate the considerable per-iteration linear algebra

overhead incurred by ANATRA. Negotiating between the theory and practice of these model update procedures involves nontrivial research effort. We are also interested in extending ANATRA with adaptive sampling techniques appropriate for stochastic optimization, such as those employed in ASTRO-DF [30]. While the assumptions made in Definition 1 did not require oracles to be an unbiased estimator of a ground truth function, there is a significant stochastic component to each noisy function evaluation done on a quantum computer. As long as the hardware error does not dominate the stochastic error, stochastic optimization (and hence adaptive sampling) may be appropriate. Opportunities exist for developing techniques to distinguish between stochastic and hardware noise, so that adaptive sampling may be effectively and judiciously performed in the VQA setting; a step towards such judicious detection can be found in [52]. The application of ANATRA to other noise settings is also of interest. For example, Definition 1 established a *global* property for oracles in the sense that ϵ_f was a constant applicable to all of \mathcal{R}^d . However, as can be seen in Line 1 of Algorithm 3, ANATRA was designed assuming ϵ_f is in fact a *local* constant, intended to be relevant only on a trust region in each iteration. In problem settings where noise is known to be nonconstant with respect to problem parameters, such as many VQA settings (see, e.g., Zhang et al. [53] and references therein), a potential extension of ANATRA might attempt to model nonconstant noise. This can be done, for instance, by constructing interpolation/regression models of ϵ_f and employing the resulting noise model not only to perform Line 1 but also to modify routines for selecting \mathcal{X} to decrease the error of noisy model gradients.

Acknowledgments

This material is based upon work supported by the U.S. Department of Energy, Office of Science, National Quantum Information Science Research Centers and the Office of Advanced Scientific Computing Research, Accelerated Research for Quantum Computing program under contract number DE-AC02-06CH11357.

A Algorithm for generating affinely independent points

Here we present an algorithm that is used in Line 7 of Algorithm 3. This algorithm is based on [37][Algorithm 4.1]. Algorithm 4 begins by computing the set of displacements of each point in \mathcal{X} from the center point, $x^0 = \theta_k$, and initializes an empty set of points \mathcal{Y} and a trivial subspace $Z = \mathcal{R}^d$. One displacement at a time, the algorithm checks whether the projection onto Z (denoted \mathbf{Proj}_Z) of a scaled displacement is sufficiently bounded away from zero (that is, the method checks whether the displacement is not sufficiently close to being orthogonal to Z). If the projection is sufficiently large, then the displacement is added to the set \mathcal{Y} , and the subspace Z is updated to be the null space to the span of the displacement vectors in \mathcal{Y} , denoted $\mathbf{Null}(\mathbf{Span}(\mathcal{Y}))$. After looping over all p points, Algorithm 4 returns the union of x^0 , the $x^i \in \mathcal{X}$ such that d^i was added to \mathcal{Y} , and the set $\{x^0 + \mathbf{Basis}(Z)\}$, where $\mathbf{Basis}(Z)$ denotes an arbitrary basis for Z . In our implementation, and as intended in [37], all of these projections and null space operations are

handled via a QR factorization with insertions, and the final basis for Z is taken as appropriate columns of the orthogonal Q factor. When we call [Algorithm 4](#) from [Algorithm 3](#), the choice of \mathcal{X} , c_s , and Δ_k is transparent. We set $\tau = 10^{-5}$.

Algorithm 4: Generating a set of affinely independent points

Input: Set of points $\mathcal{X} = \{x^0, x^1, \dots, x^p\} \subset \mathcal{R}^d$, constants $c_s \geq 1$, $\tau \in (0, 1/c_s]$, trust region Δ_k .

- 1 Set $\mathcal{D} := \{d^i = x^i - x^0 : i = 1, \dots, p\}$.
- 2 Initialize $\mathcal{Y} = \emptyset$, $Z = \mathcal{R}^d$.
- 3 **for** $i = 1, \dots, p$ **do**
- 4 **if** $\left| \text{Proj}_Z \left(\frac{1}{c_s \Delta_k} d^i \right) \right| \geq \tau$ **then**
- 5 $\mathcal{Y} \leftarrow \mathcal{Y} \cup \{d^i\}$
- 6 $Z \leftarrow \text{Null}(\text{Span}(\mathcal{Y}))$
- 7 $\mathcal{X} \leftarrow \{x^0\} \cup \{x^i : d^i \in \mathcal{Y}\} \cup \{x^0 + \text{Basis}(Z)\}$.

References

- [1] M. Cerezo, Andrew Arrasmith, Ryan Babbush, Simon C. Benjamin, Suguru Endo, Keisuke Fujii, Jarrod R. McClean, Kosuke Mitarai, Xiao Yuan, Lukasz Cincio, and Patrick J. Coles. Variational quantum algorithms. *Nature Reviews Physics*, 3(9):625–644, August 2021. doi:[10.1038/s42254-021-00348-9](https://doi.org/10.1038/s42254-021-00348-9).
- [2] Jarrod R McClean, Jonathan Romero, Ryan Babbush, and Alán Aspuru-Guzik. The theory of variational hybrid quantum-classical algorithms. *New Journal of Physics*, 18(2):023023, February 2016. doi:[10.1088/1367-2630/18/2/023023](https://doi.org/10.1088/1367-2630/18/2/023023).
- [3] Edward Farhi, Jeffrey Goldstone, and Sam Gutmann. A quantum approximate optimization algorithm. *arXiv:1411.4028*, 2014. doi:[10.48550/arXiv.1411.4028](https://doi.org/10.48550/arXiv.1411.4028).
- [4] Alberto Peruzzo, Jarrod McClean, Peter Shadbolt, Man-Hong Yung, Xiao-Qi Zhou, Peter J. Love, Alán Aspuru-Guzik, and Jeremy L. O’Brien. A variational eigenvalue solver on a photonic quantum processor. *Nature Communications*, 5(1), July 2014. ISSN 2041-1723. doi:[10.1038/ncomms5213](https://doi.org/10.1038/ncomms5213).
- [5] Zhihui Wang, Stuart Hadfield, Zhang Jiang, and Eleanor G. Rieffel. Quantum approximate optimization algorithm for MaxCut: A fermionic view. *Physical Review A*, 97(2), February 2018. doi:[10.1103/physreva.97.022304](https://doi.org/10.1103/physreva.97.022304).
- [6] Ruslan Shaydulin, Phillip C. Lotshaw, Jeffrey Larson, James Ostrowski, and Travis S. Humble. Parameter transfer for quantum approximate optimization of weighted MaxCut. *ACM Transactions on Quantum Computing*, 4(3):1–15, 2023. doi:[10.1145/3584706](https://doi.org/10.1145/3584706).

- [7] Ruslan Shaydulin, Changhao Li, Shouvanik Chakrabarti, Dylan Herman, Niraj Kumar, Jeffrey Larson, Danylo Lykov, Pierre Minssen, Yue Sun, Yuri Alexeev, Matthew DeCross, Joan M. Dreiling, John P. Gaebler, Thomas M. Gatterman, Justin A. Gerber, Kevin Gilmore, Dan Gresh, Nathan Hewitt, Chandler V. Horst, Shaohan Hu, Jacob Johansen, Mitchell Matheny, Tanner Mengle, Michael Mills, Steven A. Moses, Brian Neyenhuis, Peter Siegfried, Romina Yalovetzky, and Marco Pistoia. Evidence of scaling advantage for the quantum approximate optimization algorithm on a classically intractable problem. *arXiv:2308.02342*, 2023. doi:[10.48550/arXiv.2308.02342](https://doi.org/10.48550/arXiv.2308.02342).
- [8] Abhinav Kandala, Antonio Mezzacapo, Kristan Temme, Maika Takita, Markus Brink, Jerry M. Chow, and Jay M. Gambetta. Hardware-efficient variational quantum eigensolver for small molecules and quantum magnets. *Nature*, 549(7671):242–246, September 2017. doi:[10.1038/nature23879](https://doi.org/10.1038/nature23879).
- [9] Harper R. Grimsley, Sophia E. Economou, Edwin Barnes, and Nicholas J. Mayhall. An adaptive variational algorithm for exact molecular simulations on a quantum computer. *Nature Communications*, 10(1), July 2019. doi:[10.1038/s41467-019-10988-2](https://doi.org/10.1038/s41467-019-10988-2).
- [10] Alexander J McCaskey, Zachary P Parks, Jacek Jakowski, Shirley V Moore, Titus D Morris, Travis S Humble, and Raphael C Pooser. Quantum chemistry as a benchmark for near-term quantum computers. *npj Quantum Information*, 5(1):99, 2019. doi:[10.1038/s41534-019-0209-0](https://doi.org/10.1038/s41534-019-0209-0).
- [11] Kübra Yeter-Aydeniz, Bryan T Gard, Jacek Jakowski, Swarnadeep Majumder, George S Barron, George Siopsis, Travis S Humble, and Raphael C Pooser. Benchmarking quantum chemistry computations with variational, imaginary time evolution, and Krylov space solver algorithms. *Advanced Quantum Technologies*, 4(7):2100012, 2021. doi:[10.1002/qute.202100012](https://doi.org/10.1002/qute.202100012).
- [12] Bela Bauer, Sergey Bravyi, Mario Motta, and Garnet Kin-Lic Chan. Quantum algorithms for quantum chemistry and quantum materials science. *Chemical Reviews*, 120(22):12685–12717, October 2020. doi:[10.1021/acs.chemrev.9b00829](https://doi.org/10.1021/acs.chemrev.9b00829).
- [13] Maria Schuld, Ville Bergholm, Christian Gogolin, Josh Izaac, and Nathan Killoran. Evaluating analytic gradients on quantum hardware. *Physical Review A*, 99(3), March 2019. doi:[10.1103/physreva.99.032331](https://doi.org/10.1103/physreva.99.032331).
- [14] Matt Menickelly, Yunsoo Ha, and Matthew Otten. Latency considerations for stochastic optimizers in variational quantum algorithms. *Quantum*, 7:949, 2023. doi:[10.22331/q-2023-03-16-949](https://doi.org/10.22331/q-2023-03-16-949).
- [15] Matt Menickelly, Stefan M Wild, and Miaolan Xie. A stochastic quasi-Newton method in the absence of common random numbers. *arXiv:2302.09128*, 2023. doi:[10.48550/arXiv.2302.09128](https://doi.org/10.48550/arXiv.2302.09128).
- [16] Jonas M Kübler, Andrew Arrasmith, Lukasz Cincio, and Patrick J Coles. An adaptive optimizer for measurement-frugal variational algorithms. *Quantum*, 4:263, 2020. doi:[10.22331/q-2020-05-11-263](https://doi.org/10.22331/q-2020-05-11-263).

- [17] Andrew Arrasmith, Lukasz Cincio, Rolando D Somma, and Patrick J Coles. Operator sampling for shot-frugal optimization in variational algorithms. *arXiv:2004.06252*, 2020. doi:[10.48550/arXiv.2004.06252](https://doi.org/10.48550/arXiv.2004.06252).
- [18] Andi Gu, Angus Lowe, Pavel A Dub, Patrick J Coles, and Andrew Arrasmith. Adaptive shot allocation for fast convergence in variational quantum algorithms. *arXiv:2108.10434*, 2021. doi:[10.48550/arXiv.2108.10434](https://doi.org/10.48550/arXiv.2108.10434).
- [19] Kosuke Ito. Latency-aware adaptive shot allocation for run-time efficient variational quantum algorithms. *arXiv:2302.04422*, 2023. doi:[10.48550/arXiv.2302.04422](https://doi.org/10.48550/arXiv.2302.04422).
- [20] Aram W. Harrow and John C. Napp. Low-depth gradient measurements can improve convergence in variational hybrid quantum-classical algorithms. *Physical Review Letters*, 126(14), April 2021. ISSN 1079-7114. doi:[10.1103/physrevlett.126.140502](https://doi.org/10.1103/physrevlett.126.140502). URL <http://dx.doi.org/10.1103/PhysRevLett.126.140502>.
- [21] Ruslan Shaydulin, Ilya Safro, and Jeffrey Larson. Multistart methods for quantum approximate optimization. In *Proceedings of the IEEE High Performance Extreme Computing Conference*, 2019. doi:[10.1109/hpec.2019.8916288](https://doi.org/10.1109/hpec.2019.8916288).
- [22] Jeffrey Larson, Matt Menickelly, and Stefan M. Wild. Derivative-free optimization methods. *Acta Numerica*, 28:287–404, 2019. doi:[10.1017/s0962492919000060](https://doi.org/10.1017/s0962492919000060).
- [23] Wim Lavrijsen, Ana Tudor, Juliane Müller, Costin Iancu, and Wibe De Jong. Classical optimizers for noisy intermediate-scale quantum devices. In *IEEE International Conference on Quantum Computing and Engineering*, pages 267–277. IEEE, 2020. doi:[10.1109/QCE49297.2020.00041](https://doi.org/10.1109/QCE49297.2020.00041).
- [24] Andrew R. Conn, Katya Scheinberg, and Luís N. Vicente. *Introduction to Derivative-Free Optimization*. SIAM, 2009. doi:[10.1137/1.9780898718768](https://doi.org/10.1137/1.9780898718768).
- [25] Michael J. D. Powell. The BOBYQA algorithm for bound constrained optimization without derivatives. Technical Report DAMTP 2009/NA06, University of Cambridge, 2009. URL http://www.damtp.cam.ac.uk/user/na/NA_papers/NA2009_06.pdf.
- [26] Jorge J Moré and Stefan M Wild. Estimating computational noise. *SIAM Journal on Scientific Computing*, 33(3):1292–1314, 2011. doi:[10.1137/100786125](https://doi.org/10.1137/100786125).
- [27] Ruobing Chen, Matt Menickelly, and Katya Scheinberg. Stochastic optimization using a trust-region method and random models. *Mathematical Programming*, 169(2):447–487, 2018. doi:[10.1007/s10107-017-1141-8](https://doi.org/10.1007/s10107-017-1141-8).
- [28] Jose Blanchet, Coralia Cartis, Matt Menickelly, and Katya Scheinberg. Convergence rate analysis of a stochastic trust-region method via supermartingales. *INFORMS Journal on Optimization*, 1(2):92–119, 2019. doi:[10.1287/ijoo.2019.0016](https://doi.org/10.1287/ijoo.2019.0016).

- [29] Jeffrey Larson and Stephen C. Billups. Stochastic derivative-free optimization using a trust region framework. *Computational Optimization and Applications*, 64(3):619–645, 2016. doi:[10.1007/s10589-016-9827-z](https://doi.org/10.1007/s10589-016-9827-z).
- [30] Sara Shashaani, Fatemeh S. Hashemi, and Raghu Pasupathy. ASTRO-DF: A class of adaptive sampling trust-region algorithms for derivative-free stochastic optimization. *SIAM Journal on Optimization*, 28(4):3145–3176, 2018. doi:[10.1137/15m1042425](https://doi.org/10.1137/15m1042425).
- [31] Kuo-Hao Chang, L. Jeff Hong, and Hong Wan. Stochastic trust-region response-surface method (STRONG)—A new response-surface framework for simulation optimization. *INFORMS Journal on Computing*, 25(2):230–243, May 2013. doi:[10.1287/ijoc.1120.0498](https://doi.org/10.1287/ijoc.1120.0498).
- [32] Friedrich Menhorn, Florian Augustin, Hans-Joachim Bungartz, and Youssef M. Marzouk. A trust-region method for derivative-free nonlinear constrained stochastic optimization. *arXiv:1703.04156*, 2022. doi:[10.48550/arXiv.1703.04156](https://doi.org/10.48550/arXiv.1703.04156).
- [33] Shigeng Sun and Jorge Nocedal. A trust region method for the optimization of noisy functions. *arXiv:2201.00973*, 2022. doi:[10.48550/arXiv.2201.00973](https://doi.org/10.48550/arXiv.2201.00973).
- [34] Liyuan Cao, Albert S. Berahas, and Katya Scheinberg. First- and second-order high probability complexity bounds for trust-region methods with noisy oracles. *Mathematical Programming*, July 2023. doi:[10.1007/s10107-023-01999-5](https://doi.org/10.1007/s10107-023-01999-5).
- [35] Timothy Proctor, Melissa Revelle, Erik Nielsen, Kenneth Rudinger, Daniel Lobser, Peter Maunz, Robin Blume-Kohout, and Kevin Young. Detecting and tracking drift in quantum information processors. *Nature Communications*, 11(1), October 2020. doi:[10.1038/s41467-020-19074-4](https://doi.org/10.1038/s41467-020-19074-4).
- [36] Albert S Berahas, Liyuan Cao, Krzysztof Choromanski, and Katya Scheinberg. A theoretical and empirical comparison of gradient approximations in derivative-free optimization. *Foundations of Computational Mathematics*, 22(2):507–560, 2022. doi:[10.1007/s10208-021-09513-z](https://doi.org/10.1007/s10208-021-09513-z).
- [37] Stefan M. Wild. MNH: A derivative-free optimization algorithm using minimal norm Hessians. In *Tenth Copper Mountain Conference on Iterative Methods*, 2008. URL <http://grandmaster.colorado.edu/~copper/2008/SCWinners/Wild.pdf>.
- [38] Stefan M Wild. Chapter 40: POUNDERS in TAO: Solving derivative-free nonlinear least-squares problems with POUNDERS. In *Advances and Trends in Optimization with Engineering Applications*, pages 529–539. SIAM, 2017. doi:[10.1137/1.9781611974683.ch40](https://doi.org/10.1137/1.9781611974683.ch40).
- [39] M.J.D. Powell. Least Frobenius norm updating of quadratic models that satisfy interpolation conditions. *Mathematical Programming*, 100(1), November 2003. doi:[10.1007/s10107-003-0490-7](https://doi.org/10.1007/s10107-003-0490-7).

- [40] Coralia Cartis, Jan Fiala, Benjamin Marteau, and Lindon Roberts. Improving the flexibility and robustness of model-based derivative-free optimization solvers. *ACM Transactions on Mathematical Software*, 45(3):1–41, 2019. doi:[10.1145/3338517](https://doi.org/10.1145/3338517).
- [41] Sébastien Le Digabel. Algorithm 909: NOMAD: Nonlinear optimization with the MADS algorithm. *ACM Transactions on Mathematical Software*, 37(4):1–15, February 2011. doi:[10.1145/1916461.1916468](https://doi.org/10.1145/1916461.1916468).
- [42] C. T. Kelley. *Implicit Filtering*. Society for Industrial and Applied Mathematics, 2011. doi:[10.1137/1.9781611971903](https://doi.org/10.1137/1.9781611971903).
- [43] Waltraud Huyer and Arnold Neumaier. SNOBFIT – Stable noisy optimization by branch and fit. *ACM Transactions on Mathematical Software*, 35(2):1–25, July 2008. doi:[10.1145/1377612.1377613](https://doi.org/10.1145/1377612.1377613).
- [44] P. Gilmore and C. T. Kelley. An implicit filtering algorithm for optimization of functions with many local minima. *SIAM Journal on Optimization*, 5(2):269–285, May 1995. doi:[10.1137/0805015](https://doi.org/10.1137/0805015).
- [45] Charles Audet and J. E. Dennis. Mesh adaptive direct search algorithms for constrained optimization. *SIAM Journal on Optimization*, 17(1):188–217, January 2006. doi:[10.1137/040603371](https://doi.org/10.1137/040603371).
- [46] Charles Audet, Kwassi Joseph Dzahini, Michael Kokkolaras, and Sébastien Le Digabel. Stochastic mesh adaptive direct search for blackbox optimization using probabilistic estimates. *Computational Optimization and Applications*, 79(1):1–34, 2021. doi:[10.1007/s10589-020-00249-0](https://doi.org/10.1007/s10589-020-00249-0).
- [47] J.C. Spall. Multivariate stochastic approximation using a simultaneous perturbation gradient approximation. *IEEE Transactions on Automatic Control*, 37(3):332–341, March 1992. doi:[10.1109/9.119632](https://doi.org/10.1109/9.119632).
- [48] László Gerencsér. *Rate of Convergence of Moments of Spall’s SPSA Method*, pages 67–75. Birkhäuser Boston, 1997. doi:[10.1007/978-1-4612-1980-4_7](https://doi.org/10.1007/978-1-4612-1980-4_7).
- [49] Nathan L. Kleinman, James C. Spall, and Daniel Q. Naiman. Simulation-based optimization with stochastic approximation using common random numbers. *Management Science*, 45(11):1570–1578, November 1999. doi:[10.1287/mnsc.45.11.1570](https://doi.org/10.1287/mnsc.45.11.1570).
- [50] IBMQ. IBM Quantum Documentation: SPSA, 2024. Available at <https://docs.quantum.ibm.com/api/qiskit/qiskit.algorithms.optimizers.SPSA> accessed on Jan. 12, 2024.
- [51] Qiskit Contributors. Qiskit: An open-source framework for quantum computing, 2023.
- [52] Matt Menickelly. Estimating computational noise on parametric curves. *arXiv:2401.10757*, 2024. doi:[10.48550/arXiv.2401.10757](https://doi.org/10.48550/arXiv.2401.10757).

- [53] Dan-Bo Zhang, Bin-Lin Chen, Zhan-Hao Yuan, and Tao Yin. Variational quantum eigensolvers by variance minimization. *Chinese Physics B*, 31(12):120301, 2022. doi:[10.1088/1674-1056/ac8a8d](https://doi.org/10.1088/1674-1056/ac8a8d).